2008-12

Testing and evaluation of a pen input device using an interial/magnetic sensor module

Drakopoulos, Leonidas

Monterey, California. Naval Postgraduate School

NAVAL POSTGRADUATE SCHOOL

MONTEREY, CALIFORNIA

THESIS

TESTING AND EVALUATION OF A PEN INPUT DEVICE USING AN INERTIAL/MAGNETIC SENSOR MODULE

by

Leonidas Drakopoulos

December 2008

Thesis Advisor:	Xiaoping Yun
Second Readers:	Roberto Cristi
	Marcello Romano

Approved for public release; distribution is unlimited

THIS PAGE INTENTIONALLY LEFT BLANK

REPORT DOCUMENTATION PAGE			Form Approved OMB No. 0704-0188
Public reporting burden for this collection of information is estimated to average 1 hour per response, including the time for reviewing instruction, searching existing data sources, gathering and maintaining the data needed, and completing and reviewing the collection of information. Send comments regarding this burden estimate or any other aspect of this collection of information, including suggestions for reducing this burden, to Washington headquarters Services, Directorate for Information Operations and Reports, 1215 Jefferson Davis Highway, Suite 1204, Arlington, VA 22202-4302, and to the Office of Management and Budget, Paperwork Reduction Project (0704-0188) Washington DC 20503.			
1. AGENCY USE ONLY ***(Leave blank)***	**2. REPORT DATE** December 2008	**3. REPORT TYPE AND DATES COVERED** Master's Thesis	
4. TITLE AND SUBTITLE Testing and Evaluation of a Pen Input Device Using an Inertial/Magnetic Sensor Module		**5. FUNDING NUMBERS**	
6. AUTHOR(S) Leonidas Drakopoulos			
7. PERFORMING ORGANIZATION NAME(S) AND ADDRESS(ES) Naval Postgraduate School Monterey, CA 93943-5000		**8. PERFORMING ORGANIZATION REPORT NUMBER**	
9. SPONSORING /MONITORING AGENCY NAME(S) AND ADDRESS(ES) N/A		**10. SPONSORING/MONITORING AGENCY REPORT NUMBER**	
11. SUPPLEMENTARY NOTES The views expressed in this thesis are those of the author and do not reflect the official policy or position of the Department of Defense or the U.S. Government.			
12a. DISTRIBUTION / AVAILABILITY STATEMENT Approved for public release; distribution is unlimited		**12b. DISTRIBUTION CODE**	

13. ABSTRACT (maximum 200 words)

In this thesis, the feasibility of developing a pen input device using an inertial/magnetic sensor module is investigated. The emphasis is on testing and evaluation of algorithms for computing handwriting trajectories based on accelerometer measurement data. This research starts by placing the inertial/magnetic sensor in a 2-D plane and writing alphanumeric characters. Before continuing to evaluate the 3-D writing, a calibration algorithm is implemented for computing the length between the nose of the pen input device and the point where the inertial/magnetic sensor is attached to the pen. A velocity correction algorithm is also applied by recognizing the pause phases in the writing in order to eliminate the drift in acceleration measurements and accurately reproduce handwriting trajectories. Extensive experiments conducted for 2-D and 3-D writings indicate that it is possible to develop a pen input device to track handwriting using an inertial/magnetic sensor module. However, the performance of the handwriting tracking depends on the accuracy of the sensor module and the speed of the writing motion.

14. SUBJECT TERMS Pen input device, accelerometer, handwriting, quarternion.			**15. NUMBER OF PAGES** 81
			16. PRICE CODE
17. SECURITY CLASSIFICATION OF REPORT Unclassified	**18. SECURITY CLASSIFICATION OF THIS PAGE** Unclassified	**19. SECURITY CLASSIFICATION OF ABSTRACT** Unclassified	**20. LIMITATION OF ABSTRACT** UU

NSN 7540-01-280-5500 Standard Form 298 (Rev. 2-89)
Prescribed by ANSI Std. 239-18

THIS PAGE INTENTIONALLY LEFT BLANK

Approved for public release; distribution is unlimited

TESTING AND EVALUATION OF A PEN INPUT DEVICE USING AN INERTIAL/MAGNETIC SENSOR MODULE

Leonidas Drakopoulos
Lieutenant Junior Grade, Hellenic Navy
B.S., Naval Academy in Greece, 2008

Submitted in partial fulfillment of the
requirements for the degree of

ELECTRICAL ENGINEER
AND
MASTER OF SCIENCE IN ELECTRICAL ENGINEERING

from the

NAVAL POSTGRADUATE SCHOOL
December 2008

Author: Leonidas Drakopoulos

Approved by: Xiaoping Yun
Thesis Advisor

Roberto Cristi
Second Reader

Marcello Romano
Second Reader

Jeffrey B. Knorr
Chairman, Department of Electrical and Computer Engineering

THIS PAGE INTENTIONALLY LEFT BLANK

ABSTRACT

In this thesis, the feasibility of developing a pen input device using an inertial/magnetic sensor module is investigated. The emphasis is on testing and evaluation of algorithms for computing handwriting trajectories based on accelerometer measurement data. This research starts by placing the inertial/magnetic sensor in a 2-D plane and writing alphanumeric characters. Before continuing to evaluate the 3-D writing, a calibration algorithm is implemented for computing the length between the nose of the pen input device and the point where the inertial/magnetic sensor is attached to the pen. A velocity correction algorithm is also applied by recognizing the pause phases in the writing in order to eliminate the drift in acceleration measurements and accurately reproduce handwriting trajectories. Extensive experiments conducted for 2-D and 3-D writings indicate that it is possible to develop a pen input device to track handwriting using an inertial/magnetic sensor module. However, the performance of the handwriting tracking depends on the accuracy of the sensor module and the speed of the writing motion.

THIS PAGE INTENTIONALLY LEFT BLANK

TABLE OF CONTENTS

THIS PAGE INTENTIONALLY LEFT BLANK

LIST OF FIGURES

THIS PAGE INTENTIONALLY LEFT BLANK

LIST OF TABLES

THIS PAGE INTENTIONALLY LEFT BLANK

EXECUTIVE SUMMARY

The development of Micro-Electro-Mechanical Systems (MEMS) technology has created interest in developing many kinds of input devices for desktop computers and laptop computers. This thesis research investigates the feasibility of developing a pen input device that can reproduce the handwriting trajectory of alphanumeric characters. This pen input device is small, efficient, useful and comfortable for writing. It is constructed by attaching an inertial/magnetic sensor module to a pen.

The inertial/magnetic sensor module used in this study is a MicroStrain 3DM-GX1. The sensor module contains three orthogonal accelerometers, three orthogonal magnetometers, and three orthogonal gyrometers for each axis x,y,z and operates over 360 degrees. It provides acceleration, angular rate, and magnetometer measurements while the pen tracks the alphanumeric characters.

The acceleration measurements with double integration provide the position of the pen and consequently the handwriting trajectory. The magnetometer data and the acceleration data using the factored quaternion algorithm (FQA) provide the orientation quaternion of the sensor module and consequently of the pen input device. For the handwriting tracking of alphanumeric characters in 2-D plane and 3-D space as presented in this thesis, the sensor quaternion was used instead of the quaternion provided from the FQA.

The estimated position of the pen input device must be computed in the earth coordinate system. However, the sensor module provides acceleration measurements in the sensor coordinate system. Consequently, the acceleration data must be converted to the earth coordinate system and this conversion is implemented by using the quaternion.

In this thesis, an experiment demonstrating the importance of the sensor module velocity for the reproduction of an accurate handwriting trajectory was conducted. The sensor module was placed in a 2-D plane and moved to track a straight line with three

different motion velocities. The numerical and graphical results from the experiment indicate that the accurate handwriting trajectory is accomplished only by using the sensor module with high motion velocity.

In this research, a velocity correction algorithm is also described. An experiment with the sensor module took place and indicated with graphs that prior to the sensor module motion and after the sensor module motion, the sensor module velocity is nonzero. This is an error and the integration of this error results in an inaccurate handwriting trajectory. Mathematical equations were applied for the velocity correction algorithm and after the implementation of them in Matlab, an accurate handwriting trajectory was accomplished.

A calibration algorithm is also explained in this study. The calibration algorithm is necessary for the computation of the velocity in the nose of the pen and eventually for the estimation of the position in the nose of the pen in the earth coordinate system. This algorithm provides the constant length vector between the nose of the pen input device and the point where the inertial magnetic sensor is attached to the pen. The quaternion provided from the factored quaternion algorithm (FQA) was used for the calibration algorithm. In this thesis research, the sensor module was attached to a pen at a distance of 14 cm from the nose of the pen. After the implementation of the equations that describe the calibration process in Matlab, the constant length was computed to be 14.1 cm.

Real experimental handwriting results of alphanumeric characters for handwriting tracking in 2-D plane and 3-D space are presented in this thesis research. It is observed from all the handwriting results that the reproduced handwriting trajectory is qualitatively correct and recognizable by humans. This indicates that the construction of this pen input device using an inertial/magnetic sensor for the reproduction of the handwriting trajectory of alphanumeric characters is feasible.

It is obvious that errors in the orientation quaternion will affect the accuracy of the acceleration data in the earth coordinate system. The sensor specifications state that the dynamic accuracy of the sensor is +/-2 degrees for arbitrary orientation angles. Consequently, the sensor does not provide the accurate orientation quaternion and thus of

the pen while the handwriting tracking is taking place. Therefore, the inaccurate quaternion creates errors in the acceleration data and accordingly after the double integration to the handwriting trajectory.

In this thesis, the handwriting trajectory was accomplished by using the sensor module with high motion velocity. However, the performance of tracking handwritten alphanumeric characters in 3-D space with a high sensor motion velocity is really difficult, especially for complicated alphanumeric characters. Therefore, the handwriting tracking is not accurate with the typical writing speed.

Although this thesis research shows that the development of a pen input device by using an inertial/magnetic sensor is feasible, the use of a different inertial/magnetic sensor that will be able to provide more accurate orientation quaternion and acceleration data is recommended for the accomplishment of accurate handwriting trajectories.

THIS PAGE INTENTIONALLY LEFT BLANK

ACKNOWLEDGMENTS

After the successful completion of my thesis research, the studies in the Naval Postgraduate School in Monterey, California and everything I have accomplished in my life, I would like to thank my parents Christos Drakopoulos and Anna Drakopoulou, especially my mother for her support, advice, guidance, love and care through my whole life. I also want to thank my sister Dimitra Drakopoulou for her suggestions and advices in many personal difficulties, and my brother in law Vasilios Stamatopoulos for his guidance and help while I was taking exams for the Naval Postgraduate School. I also thank my cute niece Chrisa Stamatopoulou for offering to me good luck.

Except from my family members, I also want to express my gratitude to my teacher and thesis advisor Professor Xiaoping Yun for his support, guidance and help in the difficulties that I encountered in my thesis research. He is an excellent professor, very helpful and with amazing knowledge.

Finally, I would like to thank James Calusdian. He was extremely helpful to me for using the instruments in the Lab. I would like to wish to him good luck to his studies in the PhD program.

THIS PAGE INTENTIONALLY LEFT BLANK

I. INTRODUCTION

A. BACKGROUND

Due to the recent development in Micro-Electro-Mechanical Systems (MEMS) technology, there has been an interest in developing new input devices for computers. There are various kinds of input devices available for desktop computers and laptop computers, including wireless optical mice that are very useful in everyday life. Apart from that, there is another input device for computers, which is called a pen-type input device.

A pen-type input device can reproduce the 3-D handwriting trajectory and reconstruct this handwriting trajectory to a 2-D plane. This input device can be very useful for professors who are teaching on-line courses. Professors using this kind of input device for writing words, sentences, and many alphanumeric characters will be able to reproduce this handwriting trajectory to desktop computers, laptop computers and generally to students' computers. For distance learning in the future, it will not be necessary for professors to use cameras or other recording programs, which sometimes can not show the image of the lecture clearly because of the internet connection or many times the words, sentences, and the alphanumeric characters are hidden while the professor is writing on the blackboard.

There are two types of pen input devices. There is the self-contained type and the external reference type. The external reference type requires an external source such as a particular surface that can track the position of the pen while the pen creates the writing trajectory. The self-contained type does not require any external sources, so it is more useful, comfortable, and superior than the external reference type.

There is an external reference type that uses infrared (IR) technology in order to reproduce the handwriting trajectory [1], [2]. It is very useful and successful, but its functionality has a restriction in its range of movement. That means that this pen input device can be used only in limited spaces and not in spaces such as blackboards.

Consequently, this type of pen input device can not be useful and successful for reproducing the handwriting trajectory in on-line courses or in any other applications in everyday life.

To the contrary, this thesis research presents a smart pen input device, which can also reproduce the handwriting trajectory. It is self-contained because it does not require any external devices. It is called smart because it is small, efficient, useful, comfortable for writing, and can also reproduce the handwriting trajectory everywhere without having any function restrictions such as limited spaces. This pen is equipped with a sensor, which is shown in Figure 1.

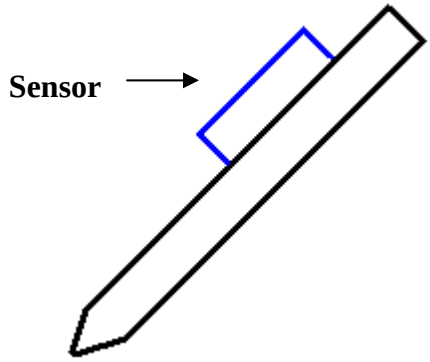

Figure 1. Smart Pen Input Device.

The sensor that is used in this thesis research is called the MicroStrain 3DM-GX1 and it is shown in Figure 2, and its specification is provided in Appendix.

Figure 2. MicroStrain 3DM-GX1 Sensor [From 3].

It is composed of three orthogonal accelerometers, three orthogonal magnetometers, and three orthogonal gyros for the three axes x,y,z and it operates over 360 degrees. The sensor collects acceleration, angular rate, and magnetometer data for the three axes x,y,z, while the pen tracks the writing trajectory. These data are provided by the accelerometers, gyros, and magnetometers of the sensor from the user's handwriting motion in 3-D space.

The acceleration data with double integration yield the position of the pen and consequently represent the handwriting trajectory along with the time. The magnetometer data with the acceleration data are used in the factored quaternion algorithm (FQA) as described in [4], in order to estimate the orientation quaternion.

The factored quaternion algorithm produces the quaternion as an output. The quaternion is used to represent the orientation of objects in 3-D space. The factored quaternion algorithm provides the orientation of the sensor and consequently the pen input device. In this thesis research, the sensor quaternion was used for the reproduction of the handwriting results in 2-D and 3-D plane as described in Chapters V and VI. The quaternion provided from the factored quaternion algorithm was used only in the calibration algorithm as described in Chapter III.

This sensor also provides angular velocities of the three axes by the three gyros, because the handwriting motion is not only a straight motion but also a rotation motion. The following chapters describe how the angular velocity ω is required in the implementation of many mathematical equations in order to represent the handwriting trajectory.

From the many mathematical equations that will be described in the following chapters in order to explain the main algorithm for the representation of the handwriting trajectory, it is obvious that the acceleration and the quaternion or the orientation of the pen are crucial for the accurate position of the pen, and consequently the reproduction of the writing trajectory.

In this thesis research, some experiments that took place proved that the sensor not only does not provide the accurate acceleration and consequently the position of the pen, but also that the velocity of the sensor motion is crucial for the accurate acceleration and position of the pen. A more detailed description for this conclusion is provided in Chapter II.

Apart from that, the position of the pen must be calculated in the earth coordinate system. By convention the earth coordinate system has the x-axis pointing to north, the y-axis pointing to east in the horizontal plane and the z-axis "straight down toward the center of the earth." [5]. Also, we define the sensor coordinate system with the x-axis, y-axis and z-axis in reference to the sensor. The earth coordinate system and the sensor coordinate system are shown in Figure 3.

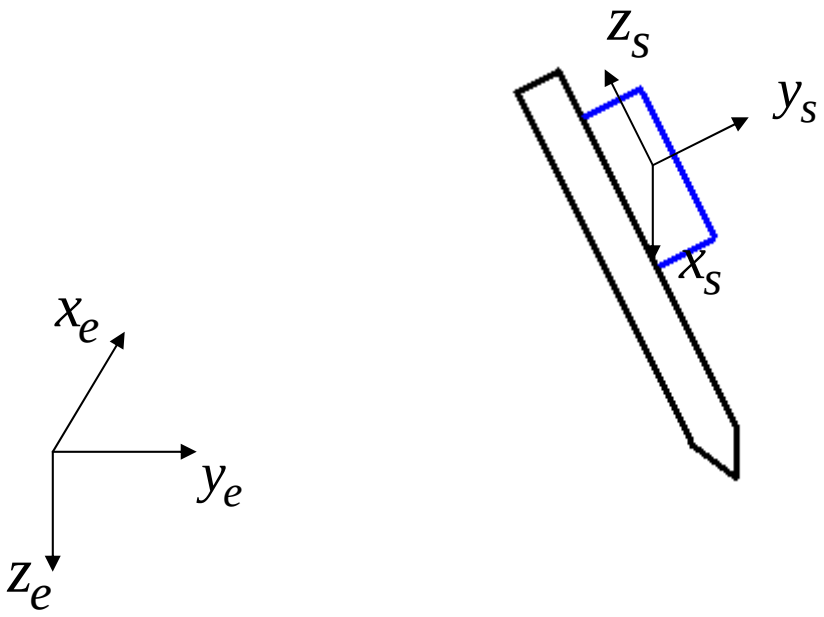

Figure 3. Sensor Coordinates x_s - y_s - z_s and Earth Coordinates x_e - y_e - z_e.

However, the acceleration data provided from the sensor are in the sensor coordinate system and consequently must be converted to the earth coordinate system. It

will be described in the main algorithm for the reproduction of the writing trajectory that this conversion can be implemented by using the quaternion. Consequently, it is obvious that if there are errors in the quaternion then the converted acceleration data in the earth coordinate system is not correct, which means that the position of the pen and the writing trajectory is not accurate.

The factored quaternion algorithm (FQA) as described in [4] does not use any angular rate measurements, and consequently it provides the accurate quaternion for only the static or slow motions of objects. It is obvious that the hand's motion and thus the sensor motion is not static and sometimes not slow when a person is writing letters, words, and sentences using a pen. Hence, the quaternion provided from the FQA is not sufficient for real-time hand motion tracking.

Besides the accuracy of the acceleration and the quaternion, there is another topic, called velocity correction that affects the accuracy of the position of the pen. The velocity data provided by the integration from the acceleration data of the sensor has an error which grows along with time. This error is called drift and happens for two main reasons. The first reason happens because of the integration of data prior to the sensor motion and after the sensor motion, or in the interval between the letters in writing a word. The other reason occurs because of the noise of the sensor. The following chapter explains that the noise of the sensor is very crucial and affects the accurate reproduction of the handwriting trajectory. Consequently, for these two main reasons, the velocity data is not correct and needs correction for the accurate position of the pen.

In this thesis research, a more detailed description with results for the topics such as quaternion, acceleration, and velocity correction that affect the accuracy of handwriting trajectory is provided in the following chapters.

Experimental handwriting results in 2-D plane and 3-D space are also included in this thesis. The handwriting trajectory in 2-D plane is reproduced when the sensor is placed on a desk as shown in Figure 4 and the performance of handwriting tracking in 3-D for the reproduction of the handwriting trajectory is implemented by attaching the sensor to a pen as shown in Figure 5.

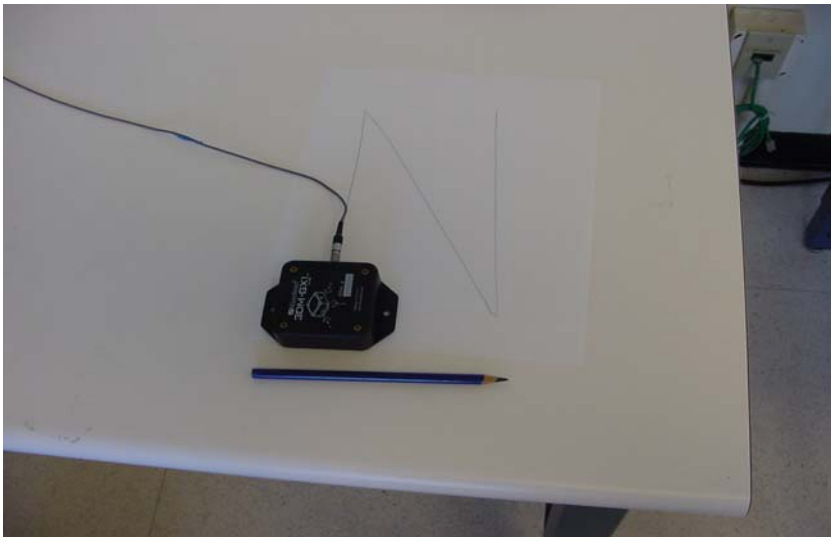

Figure 4. Handwriting Tracking in 2-D.

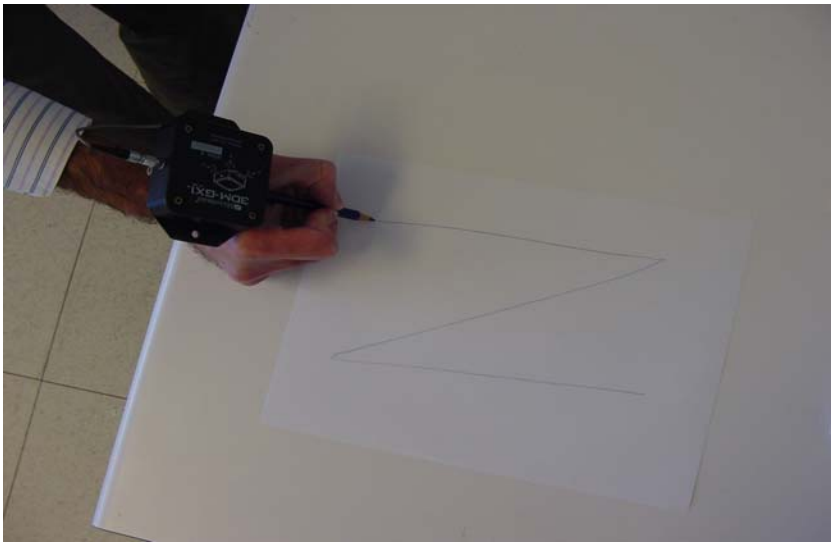

Figure 5. Handwriting Tracking in 3-D.

B. THESIS OBJECTIVES

The main goal of this thesis is to construct a pen input device using an inertial/magnetic sensor module for the reproduction of the handwriting trajectory of alphanumeric characters, which requires the following to be achieved:

- Conduct an experiment in 2-D plane using the sensor with three different motion speeds,
- Implement the calibration algorithm,
- Apply the velocity correction algorithm,
- Carry out experiments in 2-D plane and reproduction of the handwriting trajectory,
- Perform experiments in 3-D space and reproduction of the handwriting trajectory.

C. THESIS OUTLINE

Chapter II describes an experiment that took place in the 2-D plane and explains that the writing speed must be relatively high for an accurate handwriting trajectory.

Chapter III conducts the calibration algorithm for computing the constant length vector ρ_{AB} between the nose of the pen and the point where the inertial/magnetic sensor module is attached to the pen and eventually for the computation of the velocity and finally the position in the nose of the pen.

Chapter IV explains the velocity correction algorithm for eliminating the error in acceleration measurements and eventually providing accurate handwriting trajectory.

Chapter V presents experimental results of the handwriting trajectory in a 2-D plane.

Chapter VI presents experimental handwriting results for tracking alphanumeric characters in 3-D space.

The final chapter of this thesis research presents conclusions and recommendations for future work.

THIS PAGE INTENTIONALLY LEFT BLANK

II. SENSOR MOTION VELOCITY

This chapter describes an experiment and explains with results that for the MEMS sensor used in the experiment, writing speed is crucial.

A. MEASUREMENTS OF A STRAIGHT LINE

In this experiment, the MicroStrain 3DM-GX1 sensor was placed in a 2-D plane and then was moved along a straight line with three different speeds (high, medium, and slow). The actual distance of the straight line was 28 cm. The high speed of the sensor motion was computed around 42.4 cm/sec, the medium speed 15.3 cm/sec, and the slow speed 10.5 cm/sec. All these speeds of the sensor motion were calculated approximately by knowing the number of samples that was collected from the sensor, the actual distance that was tracked from the sensor, and the sampling frequency of the sensor.

The purpose of this experiment was to verify the actual distance of the straight line without using the quaternion. The accelerometer data were used only in this experiment. It is known that in order to compute the actual distance of the straight line, the accelerometer data provided from the sensor in the sensor coordinate system must be converted to the earth coordinate system. In that case, the quaternion is required to implement that conversion. However, in this experiment in order to avoid the use of the quaternion, the conversion of acceleration data from the sensor coordinate to the earth coordinate was shunned by keeping the sensor in a fixed orientation.

A low pass filter was used to the acceleration data provided from the sensor in order to smooth the accelerations. Then, the velocity correction method was applied for the interval of the sensor motion. By applying this method, the integration was implemented only for the sensor motion and not prior or after the sensor motion. In that way, the error that was inserting and growing in velocity correspondence with time was eliminated.

The acceleration data provided from the sensor and the computed distance of the straight line with high velocity of the sensor motion are shown in Figure 6.

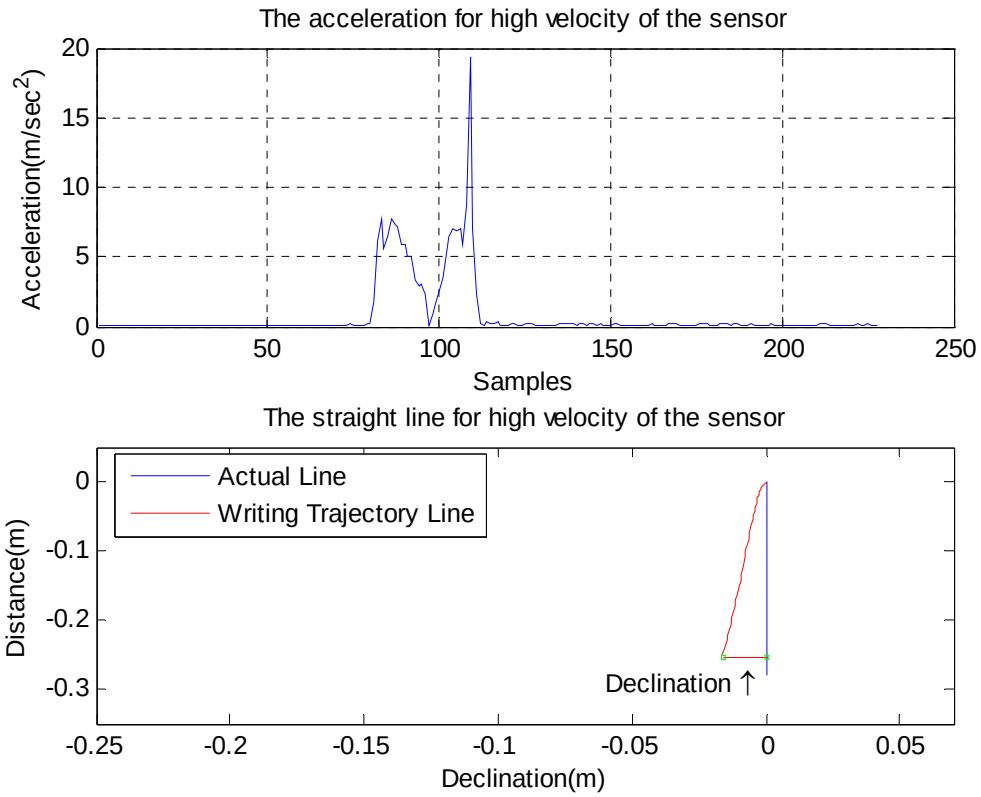

Figure 6. Results for High Speed of the Sensor Motion.

According to Figure 6, the computed distance of the straight line was 25.5 cm. The computed distance also had a declination of 1.5 cm in the horizontal axis compared with the actual vertical straight line. It is obvious from the acceleration data that the signal was very intense. The signal-to-noise ratio (SNR) was computed for that case to be 23.4484 dB.

In Figure 7 the acceleration data provided from the sensor and the computed distance of the straight line with medium velocity of the sensor motion are shown.

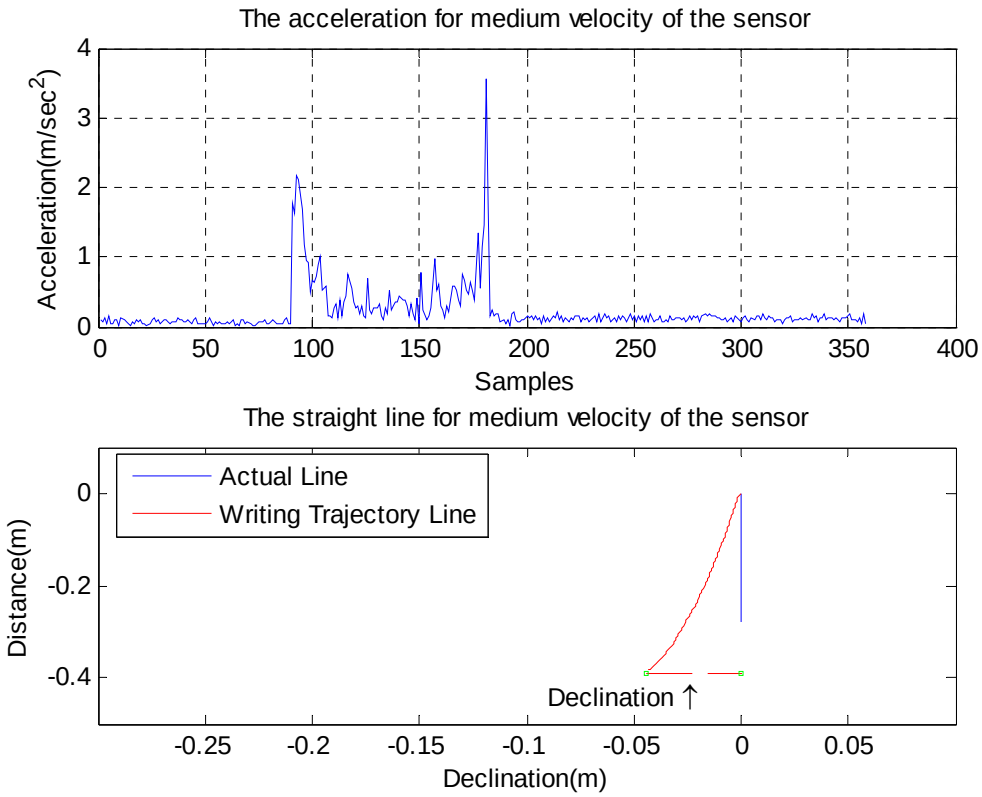

Figure 7. Results for Medium Speed of the Sensor Motion.

Regarding this figure, the distance was computed to be 39 cm, which was not so accurate. Apart from that, the declination in the horizontal axis was 4.4 cm, which was bigger than the previous case. According to the acceleration data, the signal was less intense than the previous case. The signal-to-noise ratio (SNR) was computed for this case to be 9.7138 dB.

Figure 8 presents the acceleration data provided from the sensor and the computed distance of the straight line using the slow speed for the sensor motion.

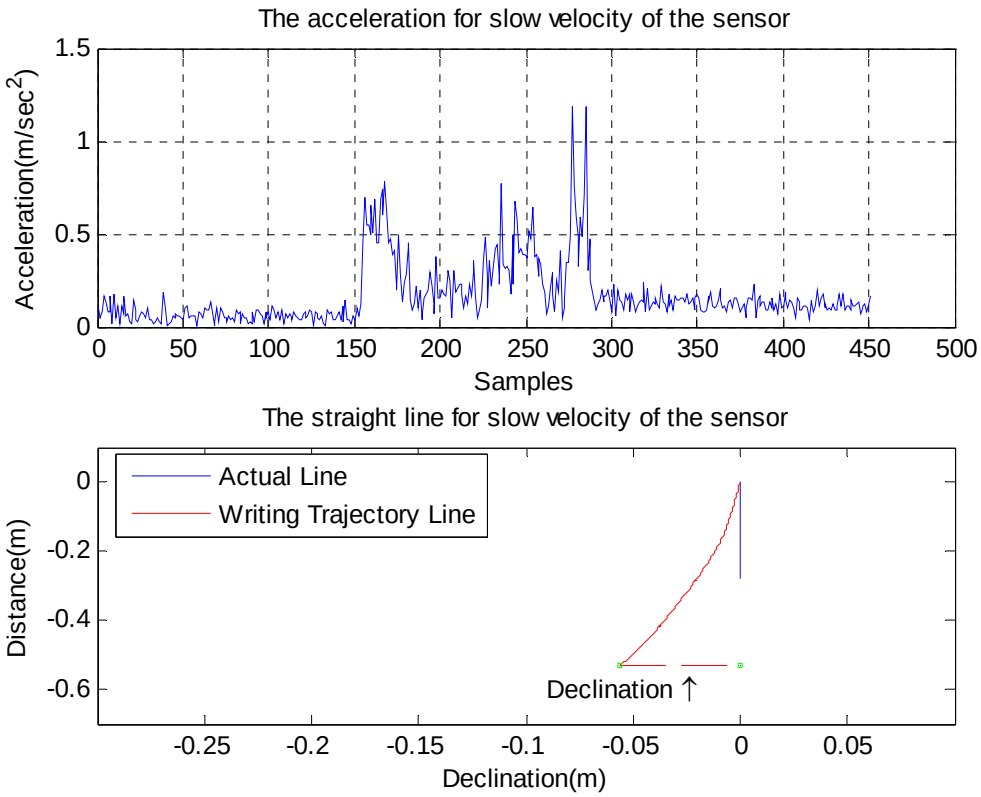

Figure 8. Results for the Slow Speed of the Sensor Motion.

In this figure, it is shown that the computed distance was 53 cm, which is unacceptable when compared with the actual. The declination as shown in Figure 8 was 5.62 cm, which was bigger than the one calculated from the first case with the sensor motion at high speed. From the acceleration data, it is noticed that the signal became weak and the noise was relatively significant. The signal-to-noise ratio (SNR) was computed in this case to be 3.3531dB.

In regards to Figures 6, 7, and 8, it is obvious that the computed distance was not only much more accurate but also had smaller declination in the horizontal axis for high velocity of the sensor motion. Apart from that, from the acceleration data it was noticed that the signal was much more intense and the noise was relatively small for high velocity of the sensor motion. This is also verified from the computed values of signal-to-noise ratio (SNR).

The following table summarizes the results from the sensor motion regarding the three different velocities.

Sensor velocities (cm/sec)	**Average value of acceleration (m/*sec*^{2})**	**Computed Distance (cm)**	**Declination (cm)**	**Distance errors (%)**
42.4	0.8282g	25.5	1.5	8.9
15.3	0.2221g	39	4.4	39.28
10.5	0.1683g	53	5.62	89.28

Table 1. Sensor Error with Three Different Velocities.

The fact that the distance errors and the declination distances grow while the velocity of the sensor motion and the average value of accelerations become smaller confirms that the accuracy in computed distances is accomplished only by using the MicroStrain 3DM-GX1 sensor with high motion velocity.

B. SUMMARY

The results of this experiment suggest that for accurate tracking at writing trajectory with the MicroStrain sensor, writing speed must be relatively high, or a more accurate accelerometer sensor must be used.

The next chapter describes the calibration algorithm for the computation of the constant length ρ_{AB} between the attached point of the sensor (A) and the nose of the pen input device point (B).

THIS PAGE INTENTIONALLY LEFT BLANK

III. CALIBRATION ALGORITHM

The calibration algorithm is needed as the first part of the algorithm in the reproduction of the handwriting trajectory for the computation of the velocity in the nose of the pen and eventually for the estimation of the position in the nose of the pen in the earth coordinate system. This algorithm provides the constant length ρ_{AB} in the sensor coordinate system between the attached point of the sensor (A) and the nose of the pen-input device point (B), as shown in Figure 9.

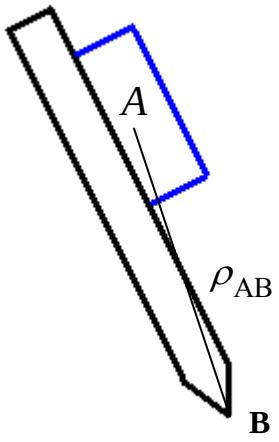

Figure 9. The Pen-input Device and the Constant Length ρ_{AB}.

The calibration process is as follows. The user holds the pen motionless against a surface and arbitrarily rotates it for a few seconds while keeping the pen tip (point B) fixed. While the user arbitrarily rotates the pen, the sensor of the pen acquires acceleration, magnetic field, and angular rate data.

The calibration algorithm provides the velocity in the nose of the pen v_B by using the following equation:

$$v_B = v_A + \omega \times \rho_{AB} \tag{1}$$

where v_B is the velocity in the nose of the pen in each axis x,y,z in the sensor coordinate system, v_A is the velocity of the sensor in each axis x,y,z in the sensor coordinate system, ω is the angular velocity in each axis x,y,z and ρ_{AB} is the constant length between points A and B.

The angular velocity ω for each axis x,y,z is provided from the sensor and the velocity v_A of the sensor for each axis x,y,z is obtained by integrating the acceleration measurement data, as shown below in Equation 2.

$$v_A = \int a\, dt \tag{2}$$

While performing the calibration, the velocity in the nose of the pen v_B is zero. Hence, in Equation (1), the unknown variable is the constant length ρ_{AB}. In Equation (1), the cross product $(\omega \times \rho_{AB})$ is replaced by the product $S_\omega \rho_{AB}$, where S_ω is the skew matrix associated with angular velocity ω for each axis x,y,z given by:

$$S_\omega = \begin{pmatrix} 0 & -\omega_Z & \omega_y \\ \omega_Z & 0 & -\omega_\chi \\ -\omega_y & \omega_\chi & 0 \end{pmatrix} \tag{3}$$

The constant length ρ_{AB} can be computed from the following equation:

$$0 = v_A + S_\omega \rho_{AB} \tag{4}$$

However, the rank of the skew matrix S_ω is 2 and it is not invertible. Therefore, the estimation of the constant length ρ_{AB} can not be computed from Equation (4) and the least-square method is used.

Let ${}^S V_A$ be a vector composed of the point A velocities in the sensor coordinate system for each axis along with the time and S is the skew matrix as described above with the angular rates to each axis along with time too.

$$ {}^{S}v_A = \begin{bmatrix} {}^{S}v_A(1) \\ . \\ . \\ . \\ {}^{S}v_A(n) \end{bmatrix} \quad (5), \qquad S = \begin{bmatrix} S_\omega(1) \\ . \\ . \\ . \\ S_\omega(n) \end{bmatrix} \quad (6) $$

where n is the number of data taken from the sensor.

Hence, the solution of the constant length ρ_{AB} is given by:

$$ \rho_{\mathrm{AB}} = -(S^T S)^{-1} S^T \, {}^{S}v_A \quad (7) $$

The implementation of the calibration algorithm in Matlab code is described in the following eight steps.

1. Load the acceleration, magnetic field, and angular rate data collected by the sensor during the calibration procedure.

2. Implement a low pass filter for the acceleration data for each axis x,y,z provided from the sensor in order to separate the gravity from the acceleration by using the following equation. This is necessary since the accelerometers of the sensor sense the gravity and the acceleration due to the motion.

$$ a_{filtered} = \alpha * a_{measured} + (1-\alpha) * a_{filtered} \quad (8) $$

where $a_{filtered}$ is the filtered accelerations, $a_{measured}$ is the measured accelerations provided from the sensor and the variable α takes a value from 0 to 1. In this thesis research, a proper value for α is 0.1073.

3. Calculate the quaternion q from the factored quaternion algorithm [4] using the acceleration and magnetometer data.

4. Convert the filtered acceleration measurements from the sensor coordinate system into the earth coordinate system using the following equation:

$$ {}^{e}a = q \; {}^{s}a \; q^{*} \quad (9) $$

where q^* is the conjugate quaternion of q and the product $(q\ {}^s a\ q^*)$ is called the quaternion product. This conversion is necessary as described in Chapter I for the estimation of the velocity and position in the nose of the pen in the earth coordinate system.

5. Obtain the velocity v_A in the earth coordinate system for the sensor in each axis x,y,z by integrating the converted filtered accelerations from step 4.

$$ {}^e v_A = \int {}^e a \, dt \tag{10}$$

6. Convert ${}^e v_A$ to ${}^s v_A$ and compute the vector ${}^s v_A$ as described in Equation (5) for all number of data n taken from the sensor.

7. Compute the skew matrix S as described in Equation (6) for all number of data n.

8. Provide the constant length ρ_{AB} by implementing Equation (7).

All the above steps in the Matlab code are implemented by using a function constant_vector=calibration(a,m,w), where a is an $n \times 4$ matrix with time and acceleration measurements, m is an $n \times 4$ matrix with time and magnetic field measurements, and ω is an $n \times 4$ matrix with time and angular rate measurements taken during the calibration procedure.

In this thesis research, the MicroStrain 3DM-GX1 sensor was attached to a pen in a distance of 14 centimeters from the nose of the pen. After the implementation of the calibration algorithm through the steps described above, in Matlab the constant length ρ_{AB} was computed to be 14.1 cm. The result is acceptable and very close to the actual distance which is 14 centimeters.

Consequently, now knowing the constant length ρ_{AB} between point A and point B, the velocity v_B in the nose of the pen is obtained from Equation (1). Finally, the

estimation for the position p_B of the nose of the pen and eventually the handwriting trajectory is obtained by integrating the velocity v_B.

$$^{e}p_B = \int {}^{e}v_B \, dt \tag{11}$$

This chapter explained the calibration algorithm for computing the constant length ρ_{AB} between the nose of the pen and the point where the inertial/magnetic sensor module is attached to the pen and eventually for the computation of the velocity and the position in the nose of the pen. The following chapter describes how the velocity v_B in the nose of the pen, before the integration and computation of position p_B, needs correction for the reasons that were explained in Chapter I.

THIS PAGE INTENTIONALLY LEFT BLANK

IV. VELOCITY CORRECTION

This chapter describes the necessity of the velocity correction in the main algorithm for the representation of the handwriting trajectory. An experiment is described in this chapter and plots are provided which prove that the velocity correction is necessary to obtain the accurate handwriting trajectory.

In this experiment, the MicroStrain 3DM-GX1 sensor was placed in a 2-D plane and then moved and tracked along a straight line of 28 cm.

In Figure 10, the acceleration plot and the velocity plot of the sensor in one axis in the sensor coordinate system are shown. The velocity of the sensor is provided from the integration of the acceleration data.

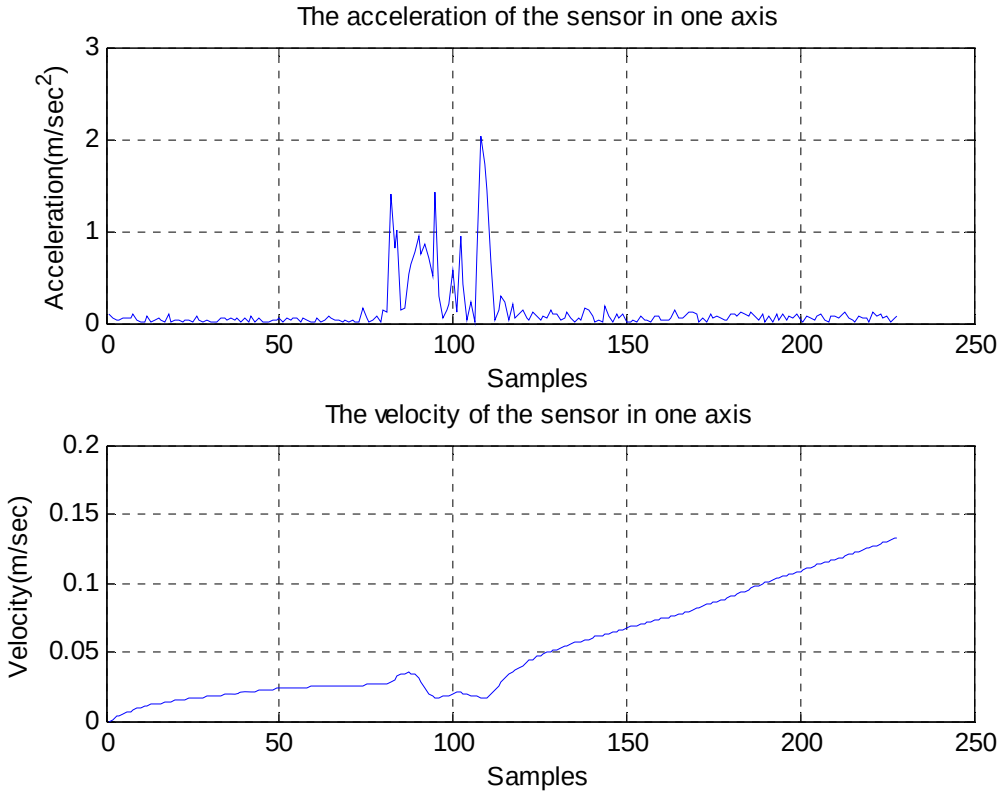

Figure 10. The Acceleration and Velocity Data of the Sensor.

It is obvious from the plot of the acceleration data that the beginning of the sensor motion occurred around the point at 80 samples and the end of the sensor motion happened around the point at 120 samples. However, it is clear from the velocity plot that the sensor's velocity is nonzero prior to the point at 80 samples and after the point at 120 samples. This is an error, because prior to the sensor motion that started around the point at 80 samples and at the end of the sensor motion that happened around the point at 120 samples, the sensor velocity should be zero. The integration of this nonzero data in order to obtain the handwriting trajectory of the straight line results in an error in the reproduction of the handwriting trajectory.

Apart from that, it was explained in Chapter II that the noise of the sensor affects the accuracy of the handwriting trajectory and consequently the position of the pen. Consequently, this error occurs not only from the integration of the nonzero data but also from the noise of the sensor. It is called drift and it is growing along with the time as it is observed in the velocity plot in Figure 10.

Figure 11 shows that the handwriting trajectory of the straight line not only is inaccurate but also has an error at the beginning and at the end of the handwriting trajectory. Consequently, the implementation of the velocity correction is needed in the main algorithm for the elimination of that error and for the reproduction of an accurate handwriting trajectory.

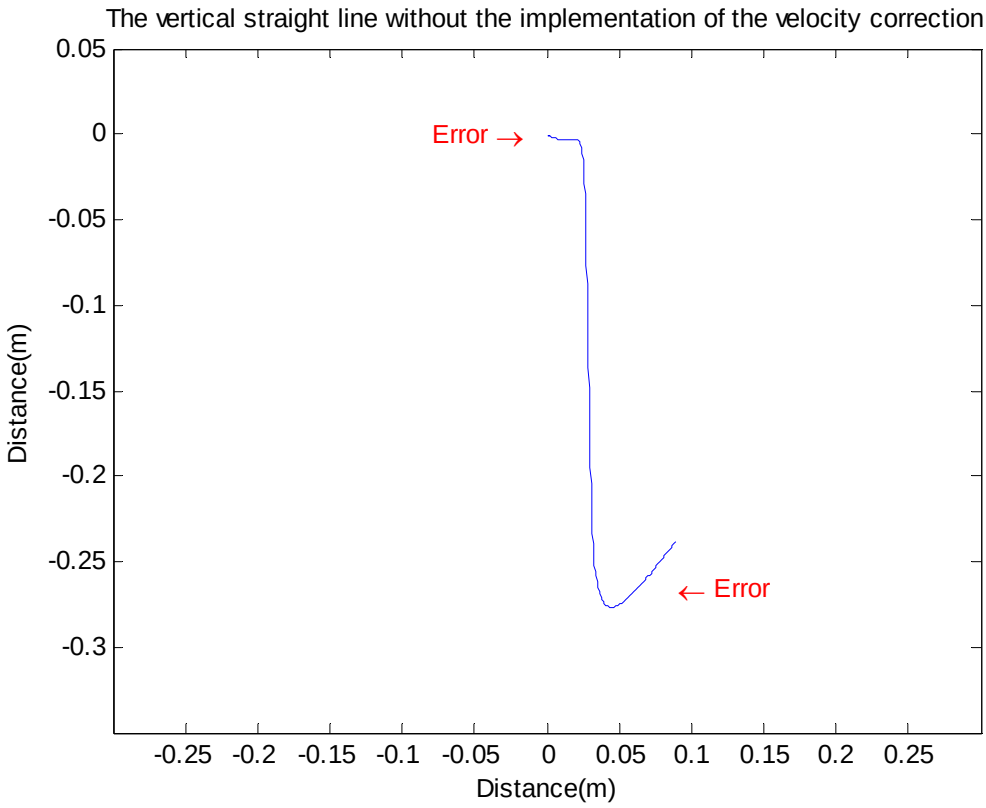

Figure 11. The Writing Trajectory of the Vertical Straight Line.

In the Matlab code, the process for the implementation of the velocity correction is the following. First, a threshold value is assigned and whenever the measured acceleration is below the threshold value the sensor is considered motionless; otherwise the sensor has motion and acquires data. Hence, in the implementation of the threshold value, the starting and ending sensor motion points are decided and the nonzero values in the sensor velocity are eliminated.

Next, the elimination of the sensor noise for the interval between the starting and ending sensor motion points is accomplished by implementing Equation (15). The proof of Equation (15) is presented below.

The measured acceleration is given by the following equation:

$$a_m(t) = a_t(t) + e \tag{12}$$

where $a_m(t)$ is the measured acceleration provided from the sensor, $a_t(t)$ is the actual acceleration, and e is the error coming from the sensor noise.

The velocity is obtained by integrating Equation (12) as follows:

$$\begin{aligned} v_m(t) &= \int a_m(t)\,dt = \int (a_t(t)+e)\,dt \\ &= v_a(t)+et \end{aligned} \tag{13}$$

where $v_a(t)$ is the actual velocity, $v_m(t)$ is the computed velocity and the term (et) means that the error, grows along with time and t is the time interval.

The end of the sensor motion occurs at time t_1 where the velocity $v_a(t)$ is zero. Hence, Equation (13) now gives the value of that error as shown below.

$$v_m(t_1) = 0 + et_1 \Rightarrow e = \frac{v_m(t_1)}{t_1} \tag{14}$$

Now, substituting Equation (14) into Equation (13) provides the corrected velocity $v_a(t)$ for the interval between the starting and ending sensor motion points.

$$v_a(t) = v_m(t) - \frac{v_m(t_1)}{t_1}t \tag{15}$$

Hence, by implementing Equation (15) in Matlab code, the velocity correction method is applied and the evidence that the effect of drift is eliminated is shown in the following figure (Figure 12).

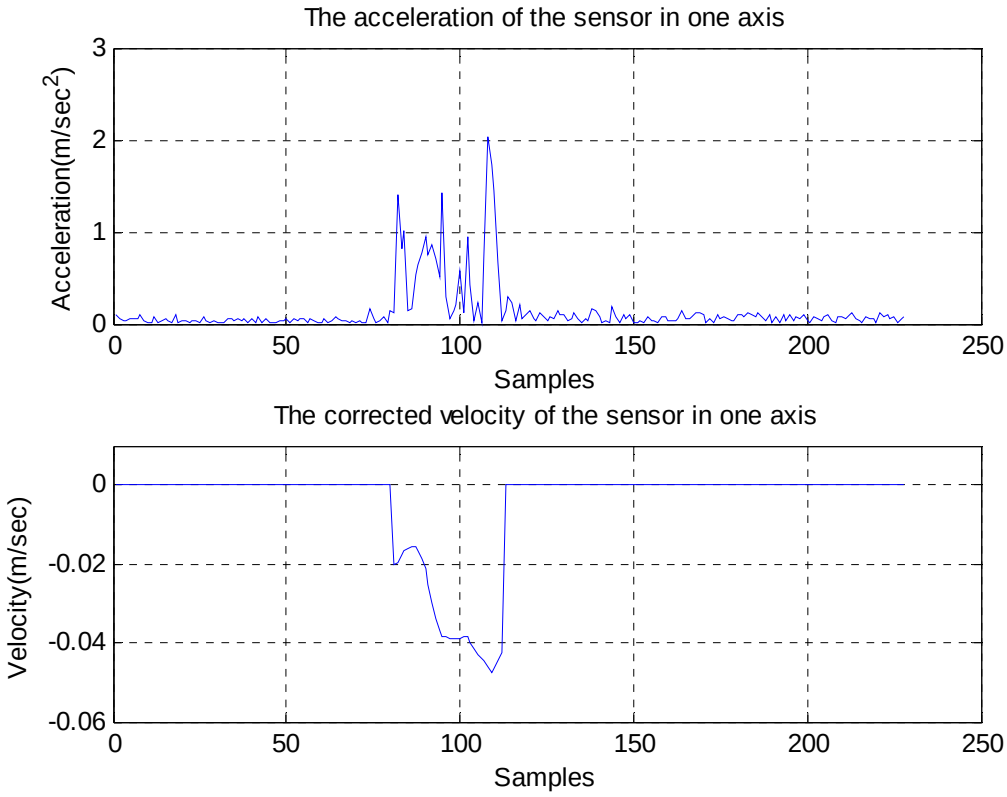

Figure 12. The Corrected Velocity of the Sensor.

It is observed from Figure 12 that prior to the sensor motion and after the sensor motion its velocity is zero.

The accuracy of the handwriting trajectory and consequently the need for the velocity correction is presented in Figure 13, where the distance of the straight line is 25.5 cm and is acceptable as the actual distance is 28 cm.

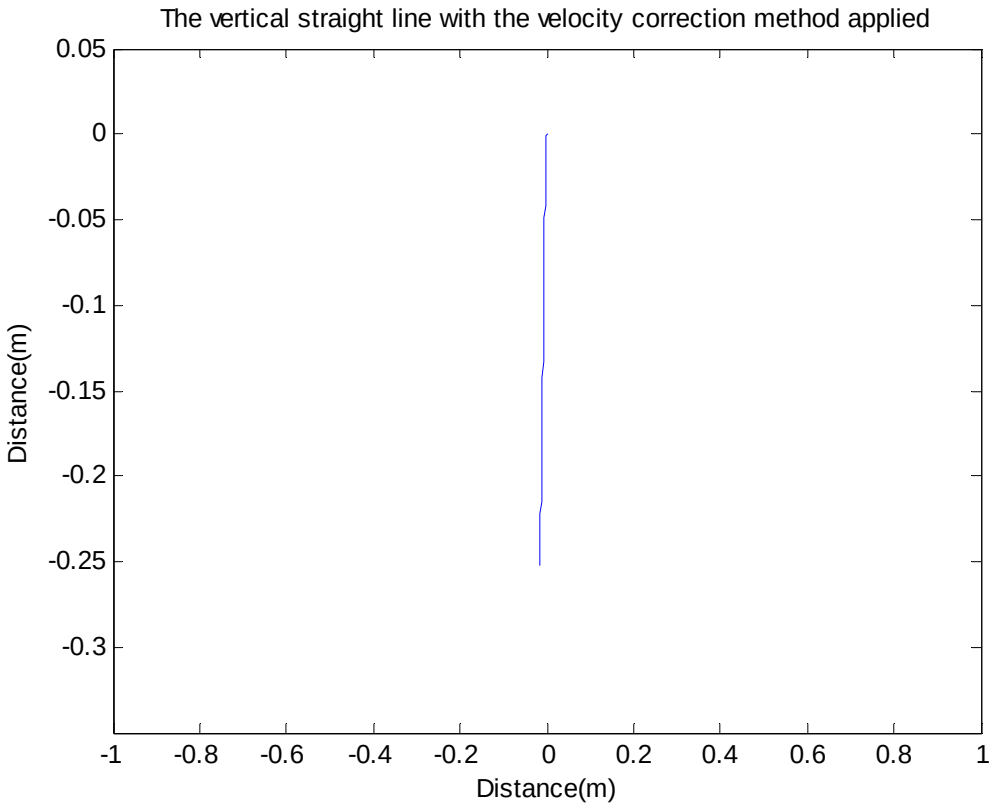

Figure 13. The Vertical Straight Line Constructed with the Velocity Correction Algorithm.

Hence, it is obvious that the implementation of the velocity correction method is necessary in the main algorithm of this thesis research for the accurate reproduction of the handwriting trajectory.

This chapter described the velocity correction algorithm in order to eliminate the drift in the acceleration measurements and to provide accurate handwriting trajectory. The next two chapters demonstrate the handwriting trajectories of alphanumeric characters for handwriting tracking in 2-D space and 3-D plane.

V. HANDWRITING TRAJECTORY IN A 2-D PLANE

This chapter presents the experimental results of the handwriting trajectory in a 2-D plane for alphanumeric characters in order to show the effectiveness of the proposed algorithm.

The MicroStrain 3DM-GX1 sensor was placed in a 2-D plane and started to move and track the alphanumeric characters with high motion velocity in order to acquire accurate handwriting trajectory as explained in Chapter II. Before the presentation of the reproduced handwriting results in a 2-D plane, it is necessary to explain the main algorithm that was implemented in Matlab in the following seven steps.

1. Loaded the acceleration and quaternion data provided by the sensor during the sensor motion for tracking the alphanumeric characters. It is necessary to mention that for these experiments the sensor quaternion was used instead of the quaternion provided from the factored quaternion algorithm (FQA).

2. Implemented a low-pass filter for the acceleration data for each axis x,y provided from the sensor in order to separate the gravity from the acceleration as explained in the calibration algorithm in Chapter III by using Equation (8). For the reproduction of the handwriting trajectory the proper value for α is 0.1073.

3. Converted the filtered accelerations measurements from the sensor coordinate system into the earth coordinate system using Equation (9) from Chapter III.

4. Obtained the velocity v_{sensor} in the earth coordinate system for the sensor in each axis x,y by integrating the converted filtered accelerations.

$$ {}^{e}v_{sensor} = \int {}^{e}a \, dt \tag{16} $$

5. Applied the velocity correction method as explained in Chapter IV in order to obtain an accurate handwriting trajectory.

6. Implemented a low pass filter for the corrected velocity from step 5 using once again Equation (8) from Chapter III in order to acquire not only an accurate but also a smooth handwriting trajectory.

7. Obtained the position of the sensor and represented the handwriting trajectory by integrating the velocity ${}^{e}v_{sensor}$ of the sensor.

$$ {}^{e}p_{sensor} = \int {}^{e}v_{sensor}\, dt \qquad (17) $$

Figures 14, 15, 16, 17, 18, 19, and 20 show the reproduced handwriting trajectory of the letters A, B, C, M, N, P, and S.

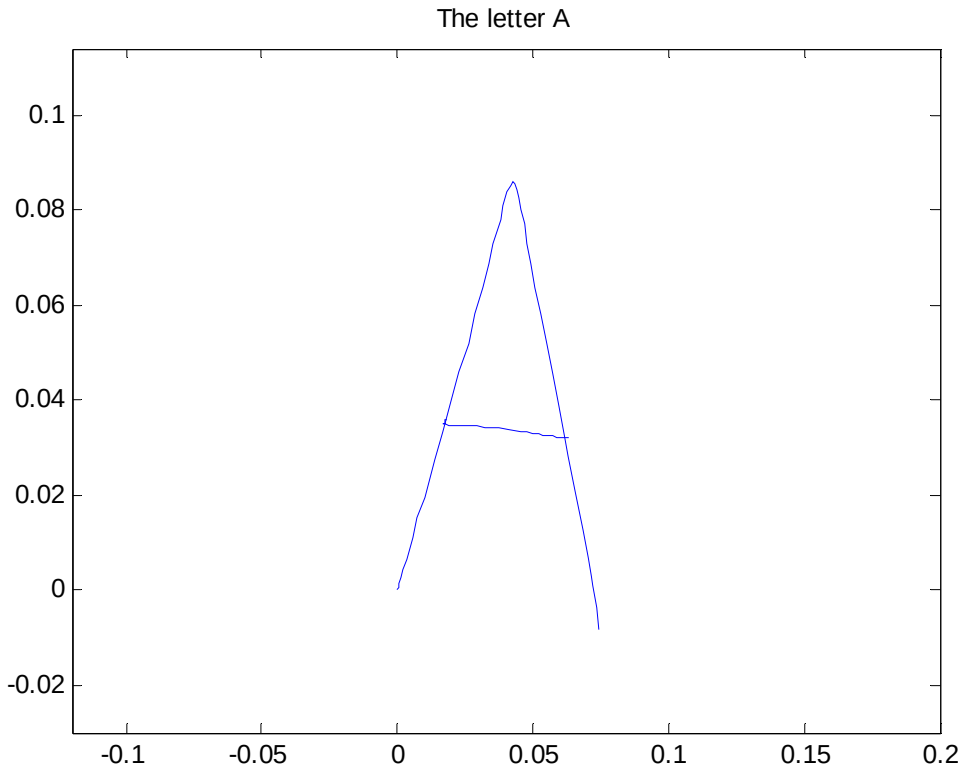

Figure 14. The Handwriting Trajectory of the Letter A, with the horizontal and vertical axis units in meters.

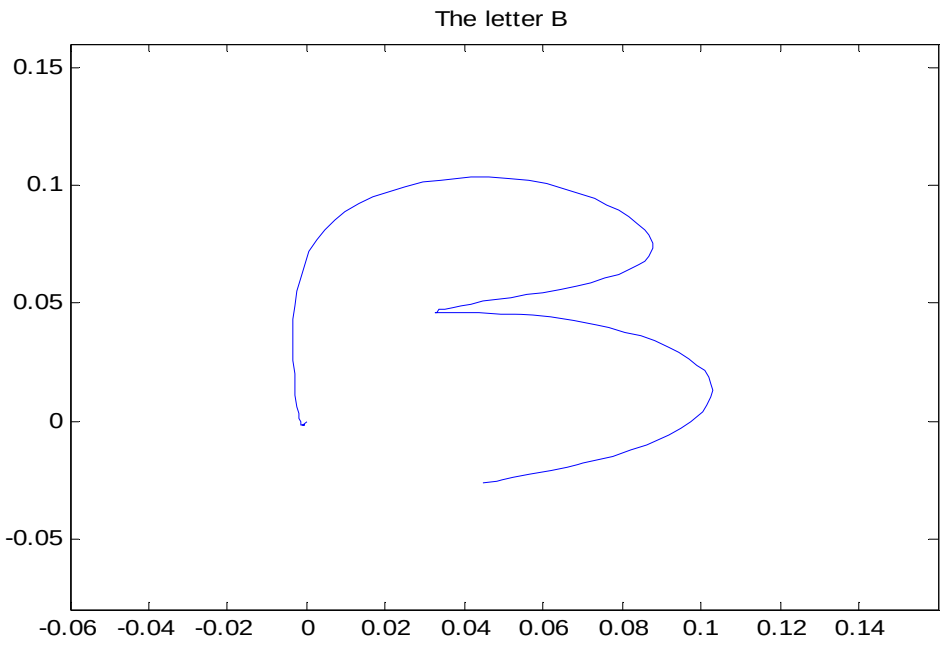

Figure 15. The Handwriting Trajectory of the Letter B, with the horizontal and vertical axis units in meters.

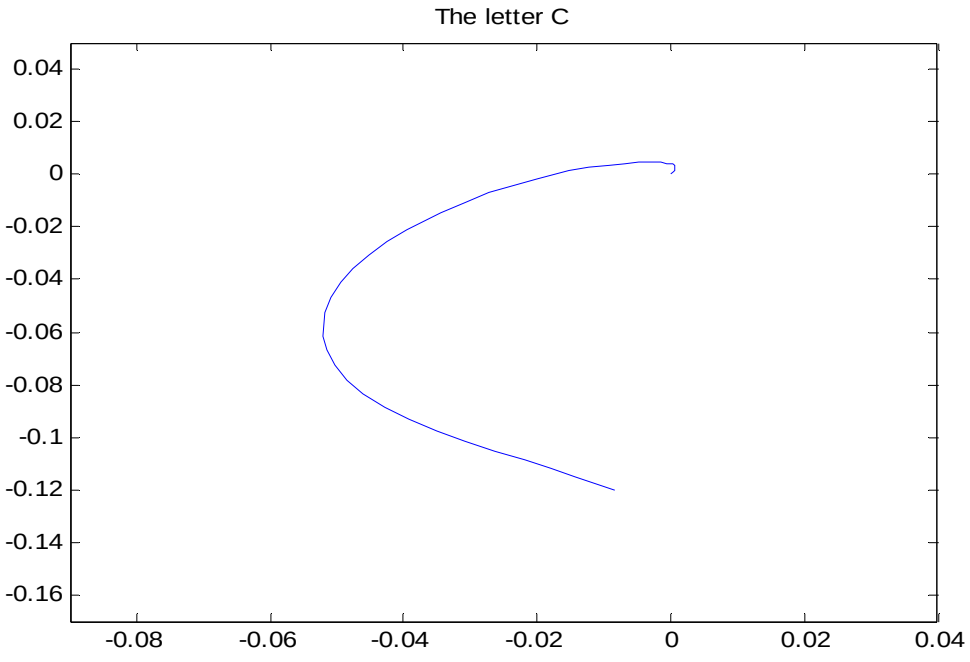

Figure 16. The Handwriting Trajectory of the Letter C, with the horizontal and vertical axis units in meters.

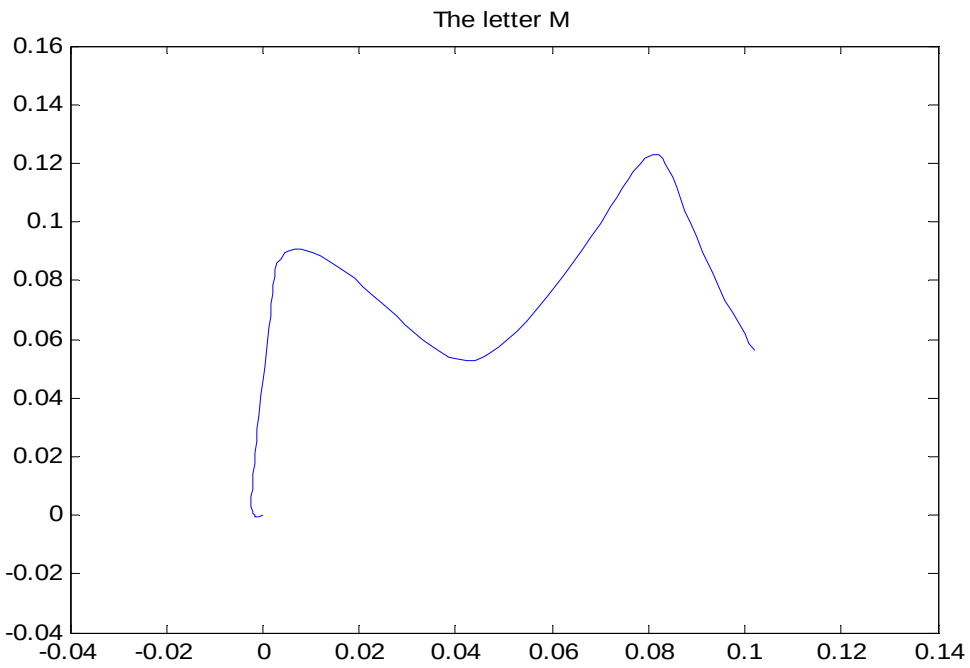

Figure 17. The Handwriting Trajectory of the Letter M, with the horizontal and vertical axis units in meters.

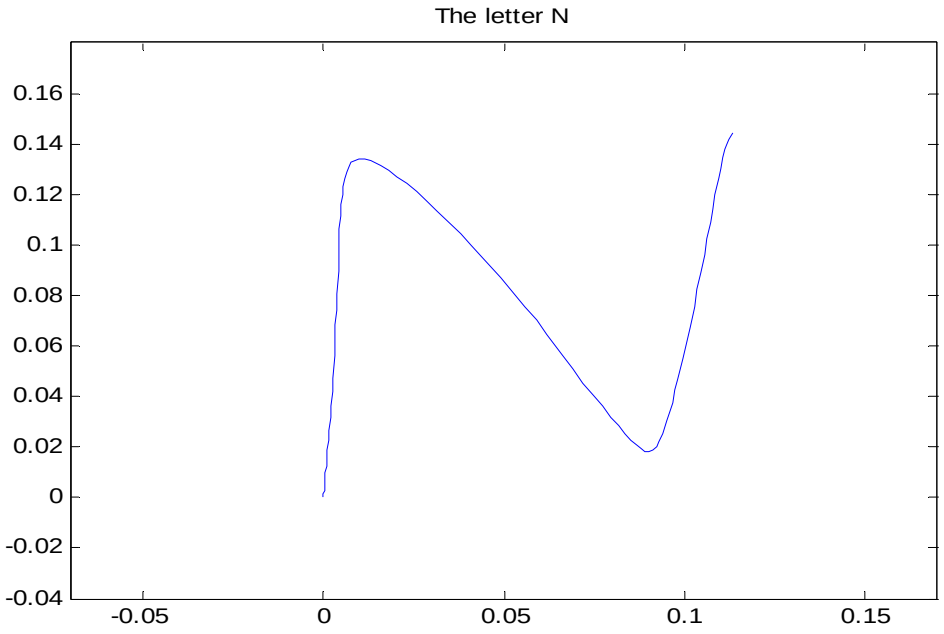

Figure 18. The Handwriting Trajectory of the Letter N, with the horizontal and vertical axis units in meters.

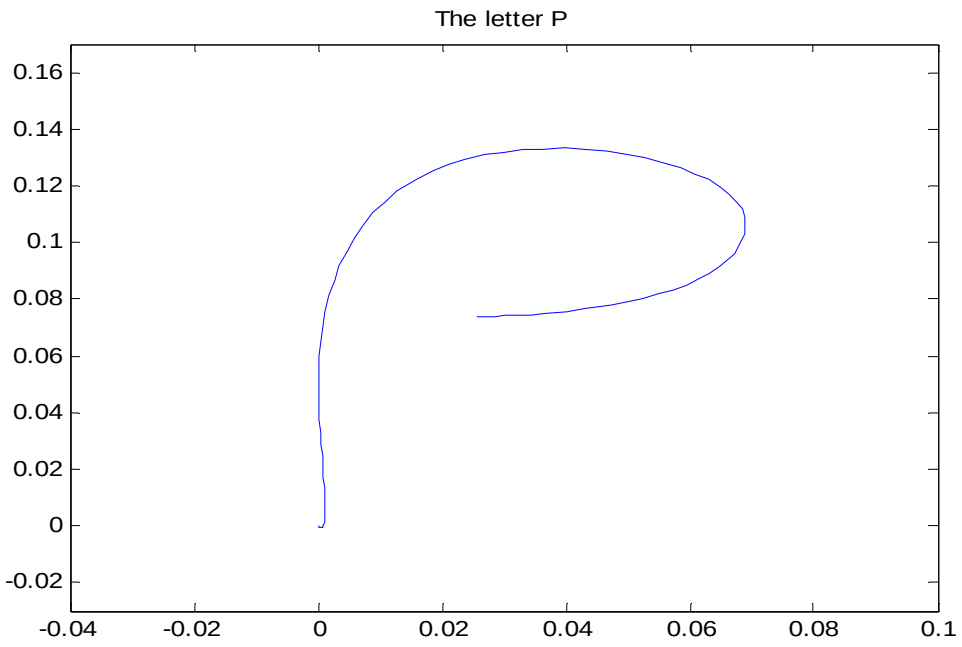

Figure 19. The Handwriting Trajectory of the Letter P, with the horizontal and vertical axis units in meters.

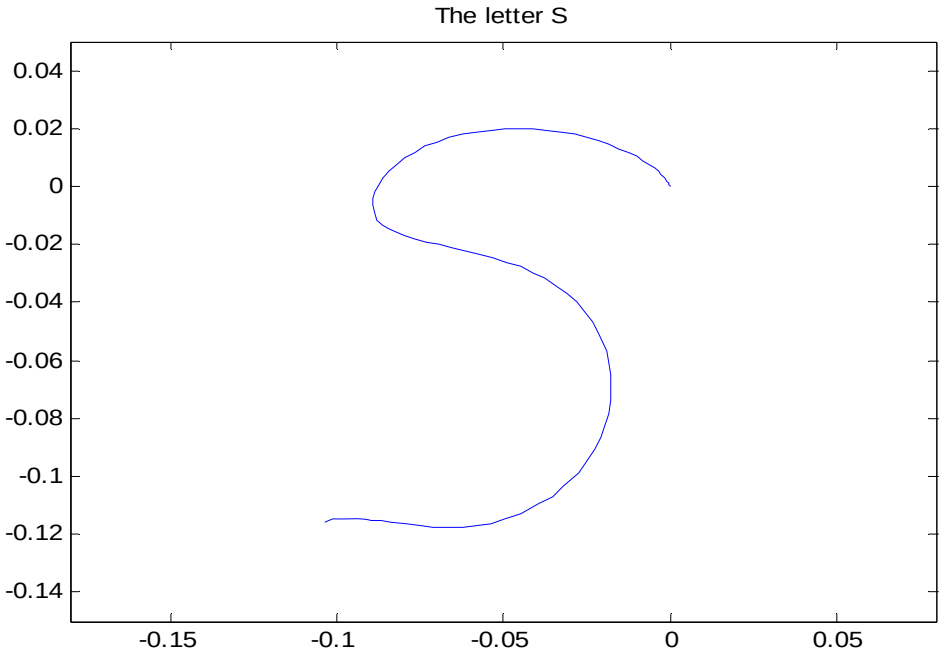

Figure 20. The Handwriting Trajectory of the Letter S, with the horizontal and vertical axis units in meters.

Figures 21, 22, 23, 24, 25, 26, 27, 28, 29, and 30 present the reproduced handwriting trajectory of the numbers 1 to 10.

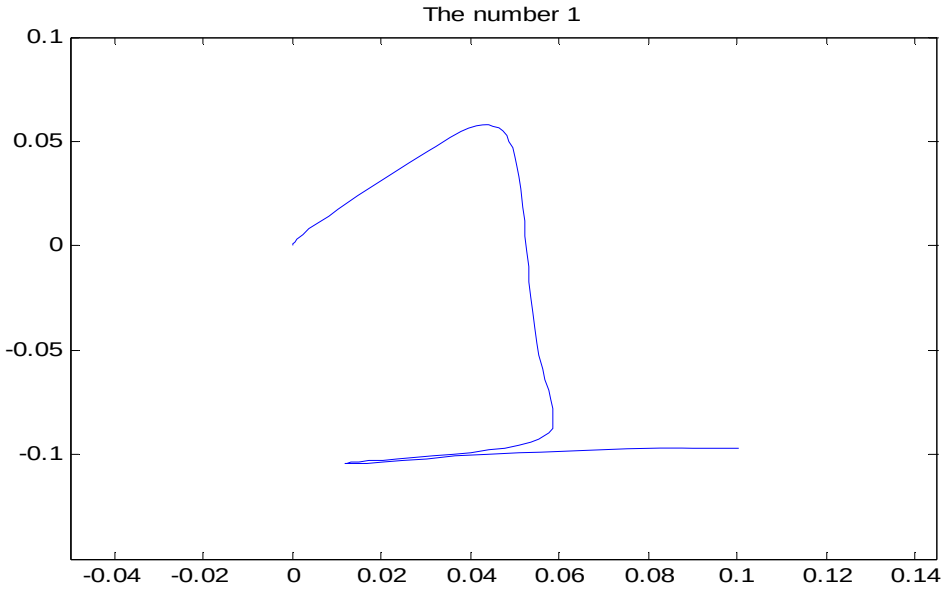

Figure 21. The Handwriting Trajectory of the Number 1, with the horizontal and vertical axis units in meters.

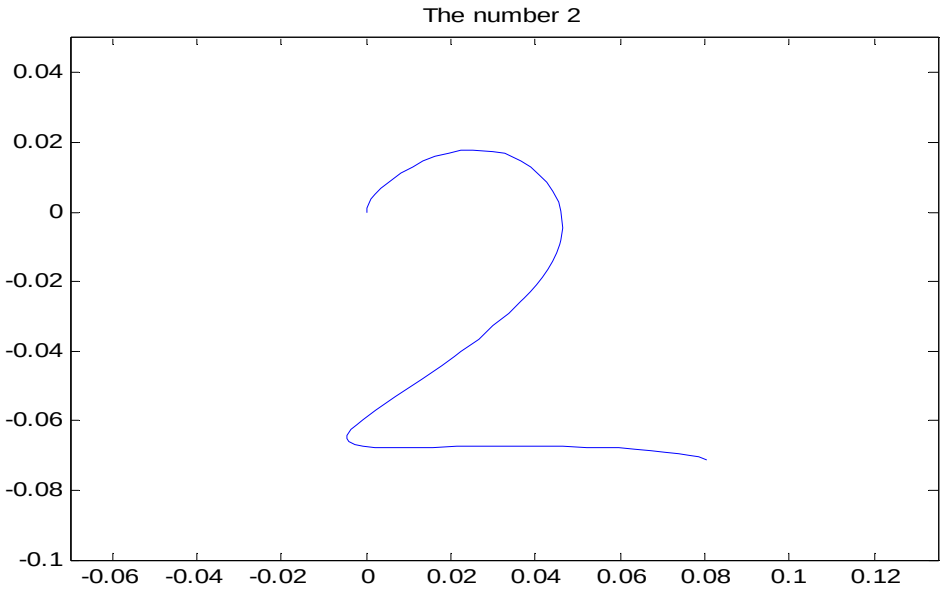

Figure 22. The Handwriting Trajectory of the Number 2, with the horizontal and vertical axis units in meters.

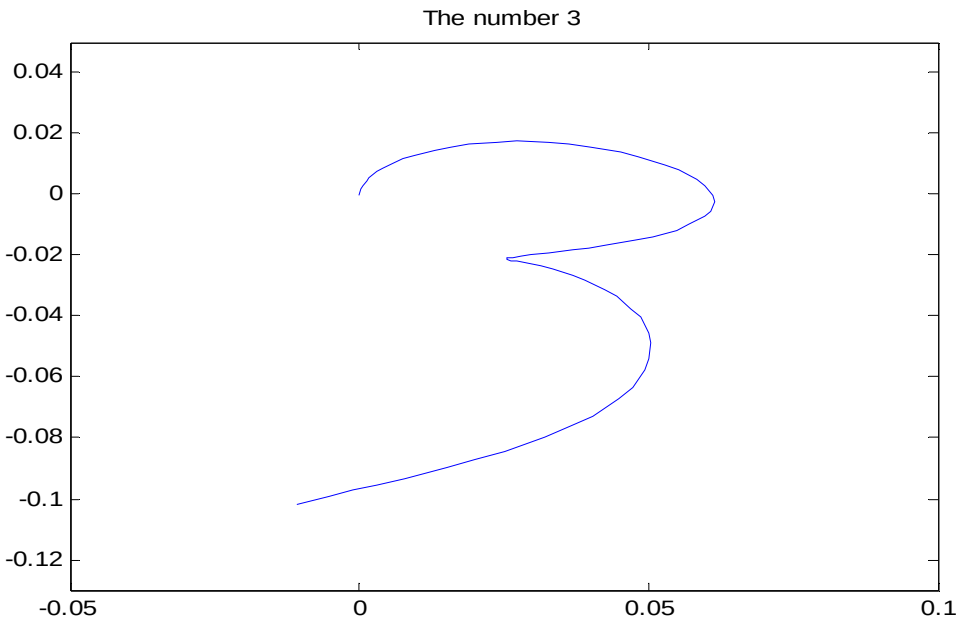

Figure 23. The Handwriting Trajectory of the Number 3, with the horizontal and vertical axis units in meters.

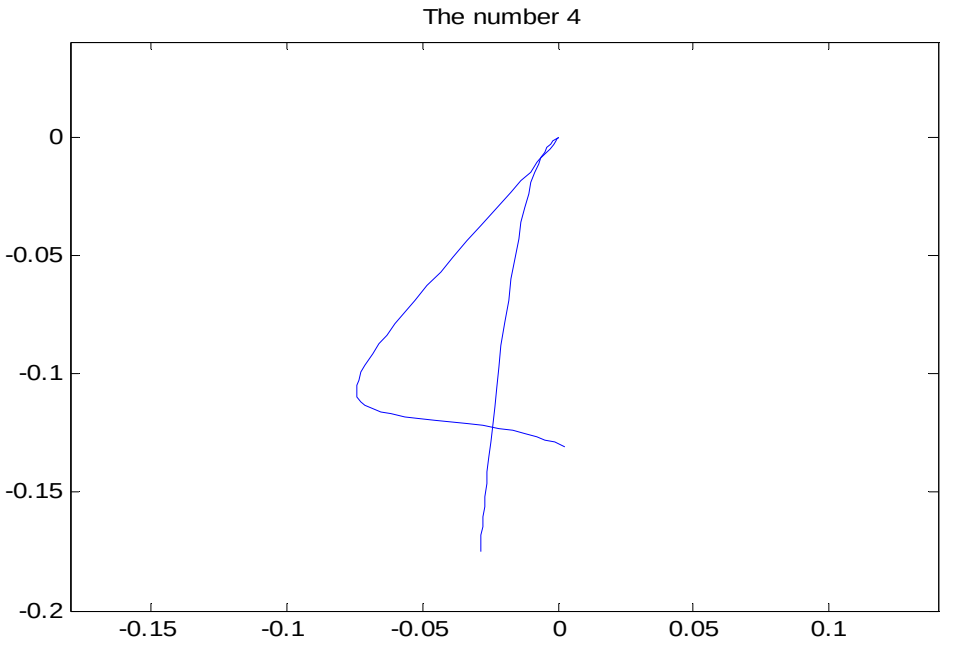

Figure 24. The Handwriting Trajectory of the Number 4, with the horizontal and vertical axis units in meters.

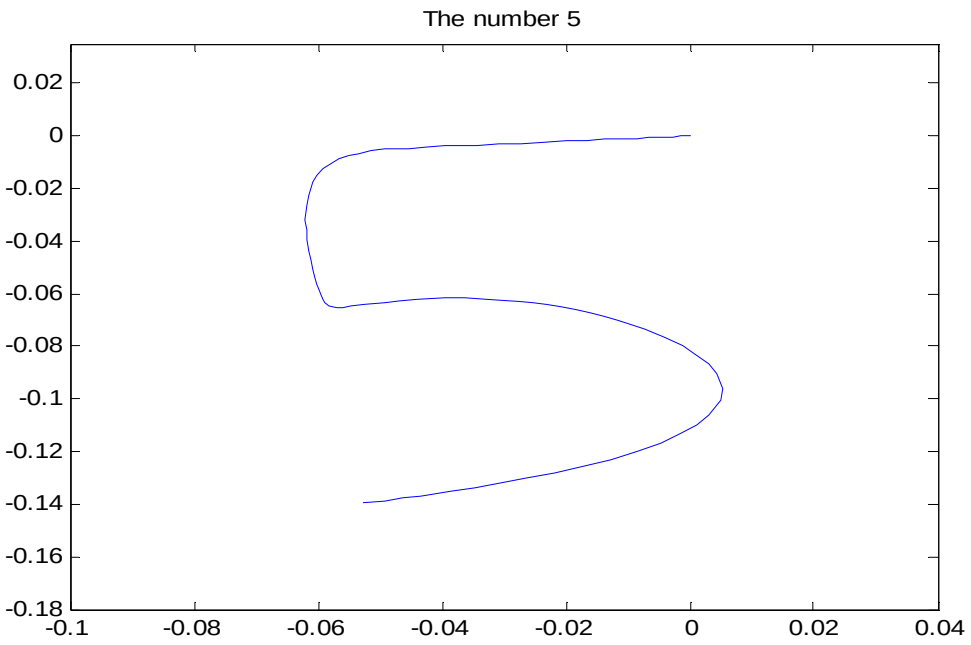

Figure 25. The Handwriting Trajectory of the Number 5, with the horizontal and vertical axis units in meters.

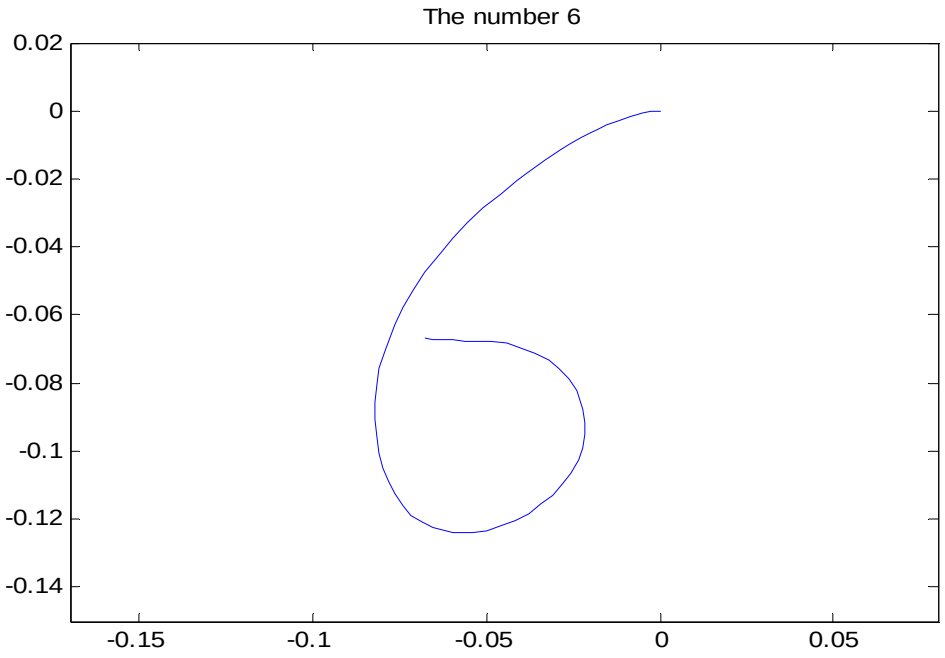

Figure 26. The Handwriting Trajectory of the Number 6, with the horizontal and vertical axis units in meters.

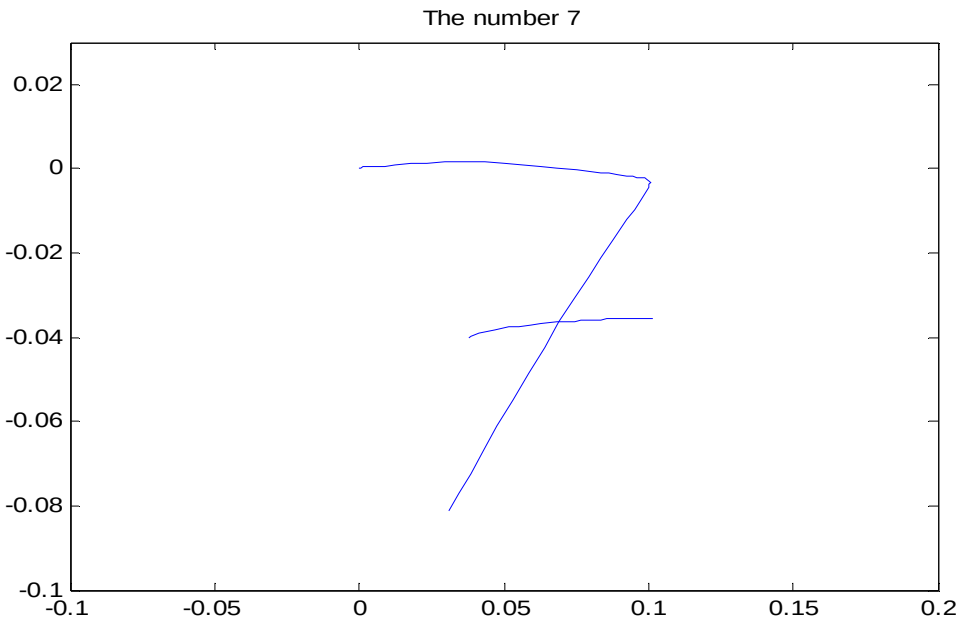

Figure 27. The Handwriting Trajectory of the Number 7, with the horizontal and vertical axis units in meters.

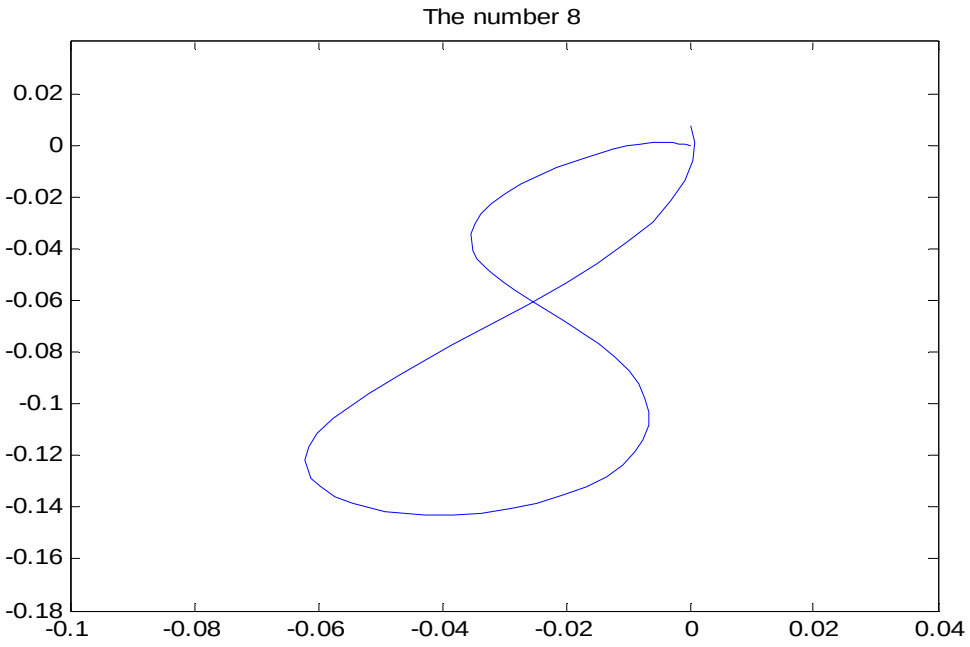

Figure 28. The Handwriting Trajectory of the Number 8, with the Horizontal and Vertical Axis Units in Meters.

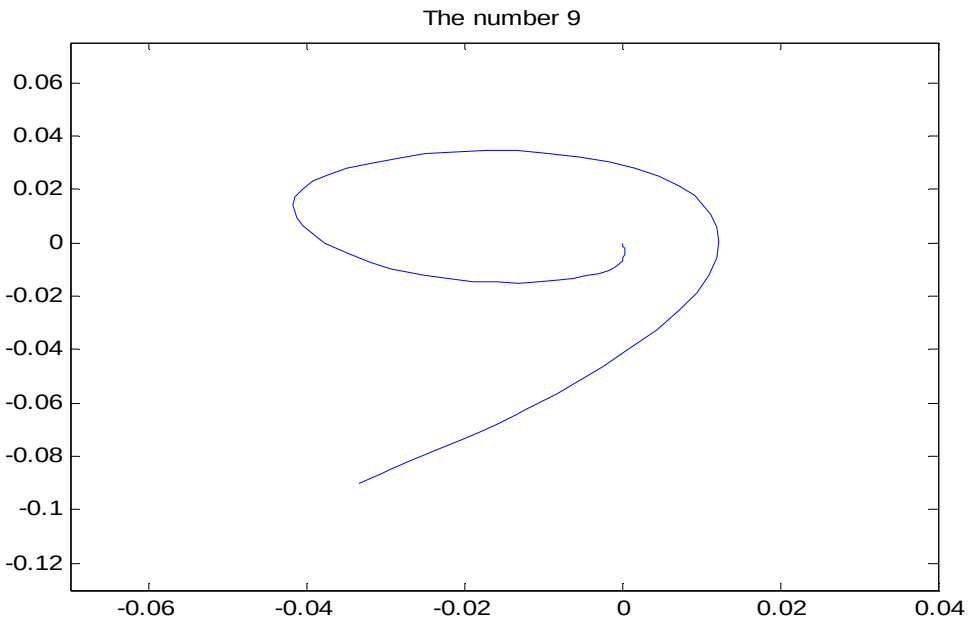

Figure 29. The Handwriting Trajectory of the Number 9, with the horizontal and vertical axis units in meters.

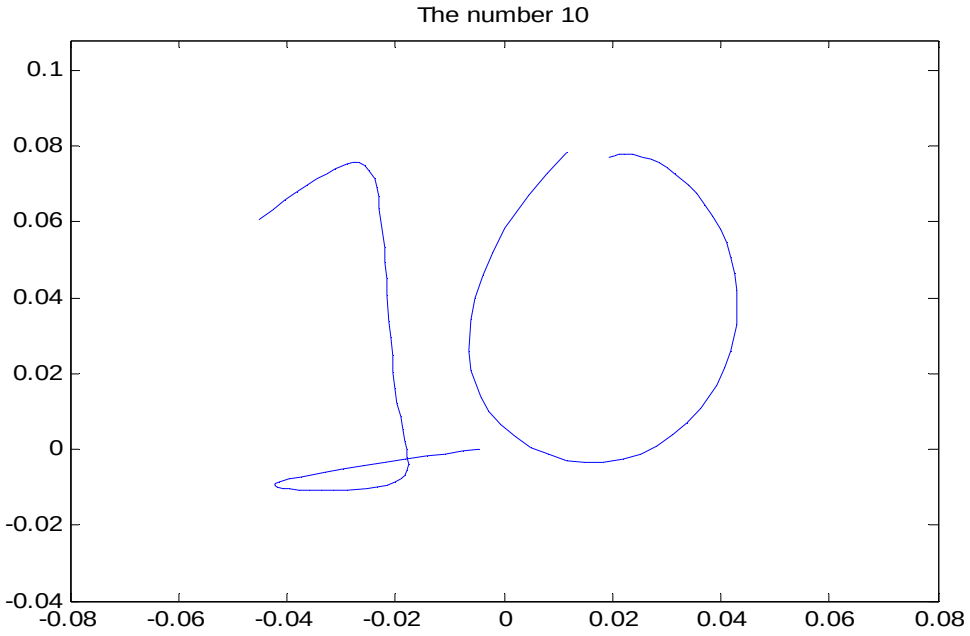

Figure 30. The Handwriting Trajectory of the Number 10, with the horizontal and vertical axis units in meters.

It is known that there are some alphanumeric characters such as the letter A and the number 7 that can be written in more than one stroke. For these cases in the main algorithm the start and end points of each stroke are found, and consequently the velocity correction method and then the integration of the corrected velocity are implemented separately for each stroke.

In this thesis research, the sensor was also tested to reproduce the handwriting trajectory of a word/acronym in a 2-D plane. The following figure (Figure 31) presents the recognizable handwriting trajectory of the word/acronym NPS.

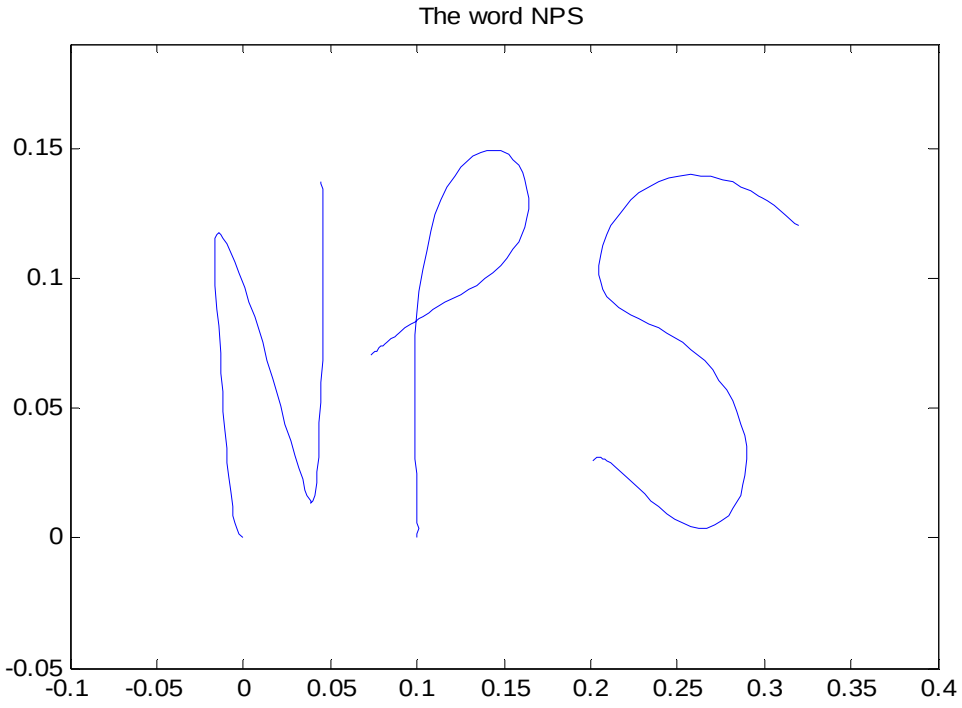

Figure 31. The Handwriting Trajectory of the acronym NPS, with the horizontal and vertical axis units in meters.

Figure 31 is evidence that the sensor can reproduce handwriting trajectories not only for letters but also for words and acronyms as well as sentences. Hence, it is obvious from all the above figures that the reproduced handwriting trajectories in a 2-D plane are sufficient and recognizable by humans.

THIS PAGE INTENTIONALLY LEFT BLANK

VI. HANDWRITING TRAJECTORY IN A 3-D SPACE

This chapter presents the experimental handwriting results for tracking alphanumeric characters in 3-D space by using the pen input device.

The MicroStrain 3DM-GX1 sensor was attached to a pen at a distance of 14 cm from the nose of the pen, and the constant length ρ_{AB} between the attached point of the sensor (A) and the nose of the pen input device (B) was computed to be 14.1 cm by implementing the calibration algorithm in Matlab as explained in Chapter III.

The main algorithm used for the reproduction of the handwriting trajectory by using the pen input device is described in the following eight steps.

1. Loaded the acceleration, quaternion, and angular rate data provided by the sensor during the pen's motion for tracking the alphanumeric characters. For these handwriting results, the sensor quaternion was also used instead of the quaternion provided from the factored quaternion algorithm (FQA).

2. Implemented a low pass filter for the acceleration data for each axis x,y,z provided from the sensor in order to separate the gravity from the acceleration as explained in the calibration algorithm in Chapter III by using Equation (8). For the reproduction of handwriting trajectories the proper value for α is 0.1073.

3. Converted the filtered accelerations measurements from the sensor coordinate system into the earth coordinate system using Equation (9) from Chapter III.

4. Obtained the velocity v_A in the earth coordinate system for the sensor in each axis x,y,z by integrating the converted filtered accelerations.

$$ {}^{e}v_A = \int {}^{e}a \, dt \tag{18} $$

5. Computed the velocity v_B in the nose of the pen in the earth coordinate system based on the sensor velocity v_A by using the following equation.

$$ {}^{e}v_B = {}^{e}v_A + q({}^{s}\omega \times {}^{s}\rho_{AB})q^{*} \tag{19} $$

where ω was the angular rate provided from the sensor and ρ_{AB} was the constant length computed from the calibration algorithm as explained in Chapter III. The quaternion rotation operator was used in order to convert the angular rate vector ω and the constant length vector ρ_{AB} from the sensor coordinate system into the earth coordinate system.

6. Applied the velocity correction algorithm in order to recognize the pause phases in writing and obtain an accurate handwriting trajectory as explained in Chapter IV.

7. Implemented a low pass filter for the corrected velocity from step 6 using Equation (8) from Chapter III in order to acquire an accurate and smooth handwriting trajectory.

8. Obtained the position in the nose of the pen in the earth coordinate system and reproduced the handwriting trajectory by integrating the corrected velocity v_B in the nose of the pen.

$$^{e}p_B = \int {}^{e}v_B \, dt \tag{20}$$

Figures 32, 33, 34, 35, 36, 37, 38, and 39 present the reproduced handwriting trajectories of the letters A, B, C, E, F, N, P, and S.

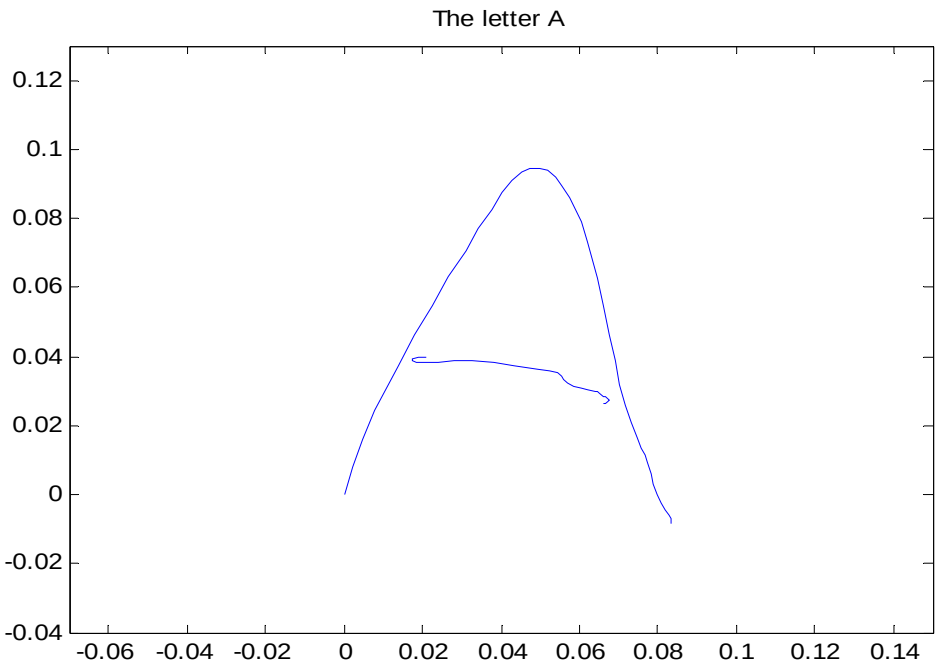

Figure 32. The Handwriting Trajectory of the Letter A, with the horizontal and vertical axis units in meters.

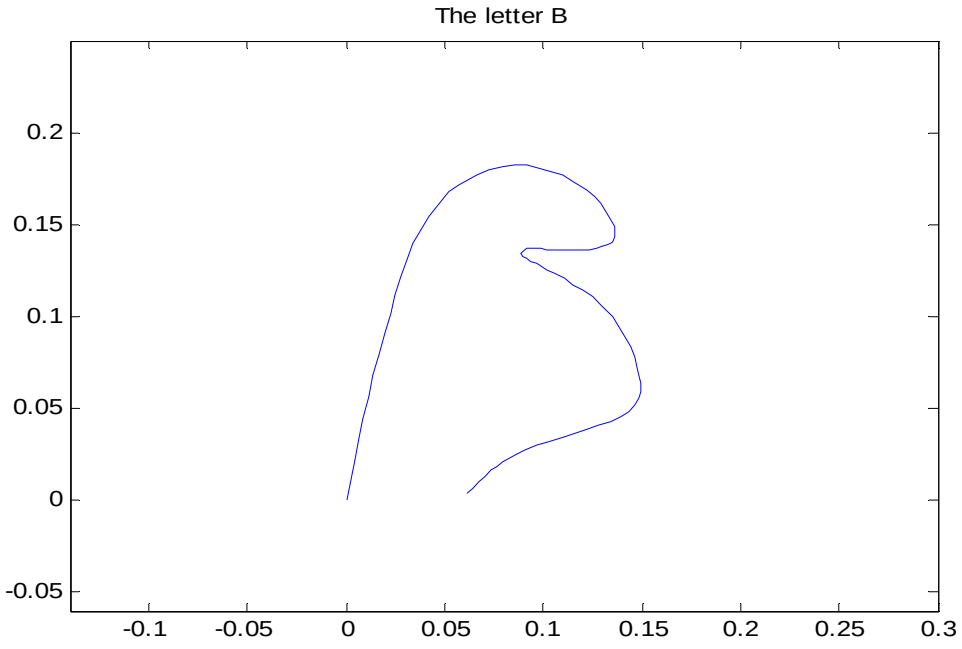

Figure 33. The Handwriting Trajectory of the Letter B, with the horizontal and vertical axis units in meters.

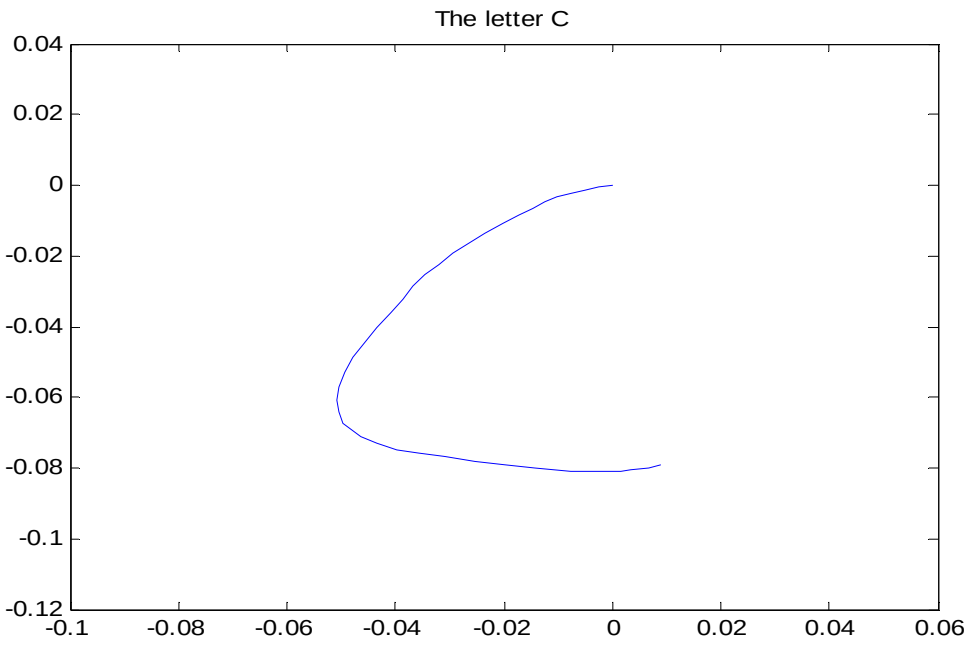

Figure 34. The Handwriting Trajectory of the Letter C, with the horizontal and vertical axis units in meters.

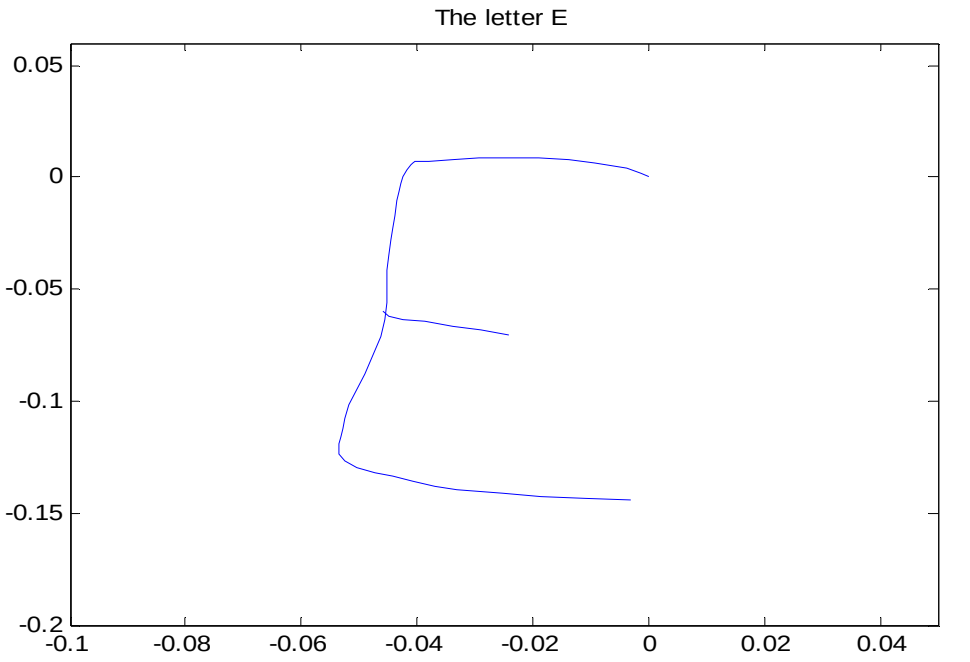

Figure 35. The Handwriting Trajectory of the Letter E, with the horizontal and vertical axis units in meters.

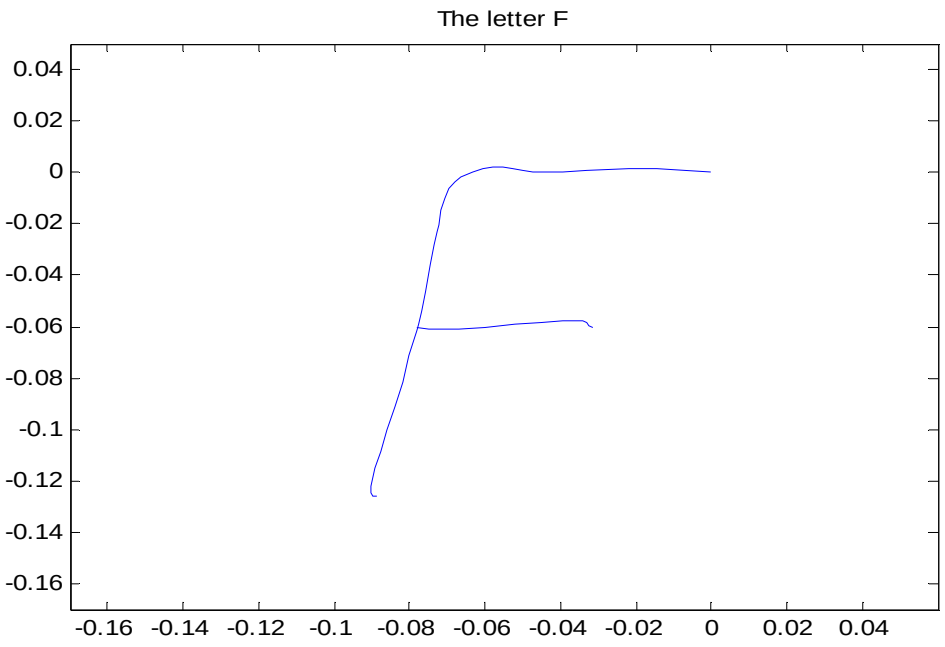

Figure 36. The Handwriting Trajectory of the Letter F, with the horizontal and vertical axis units in meters.

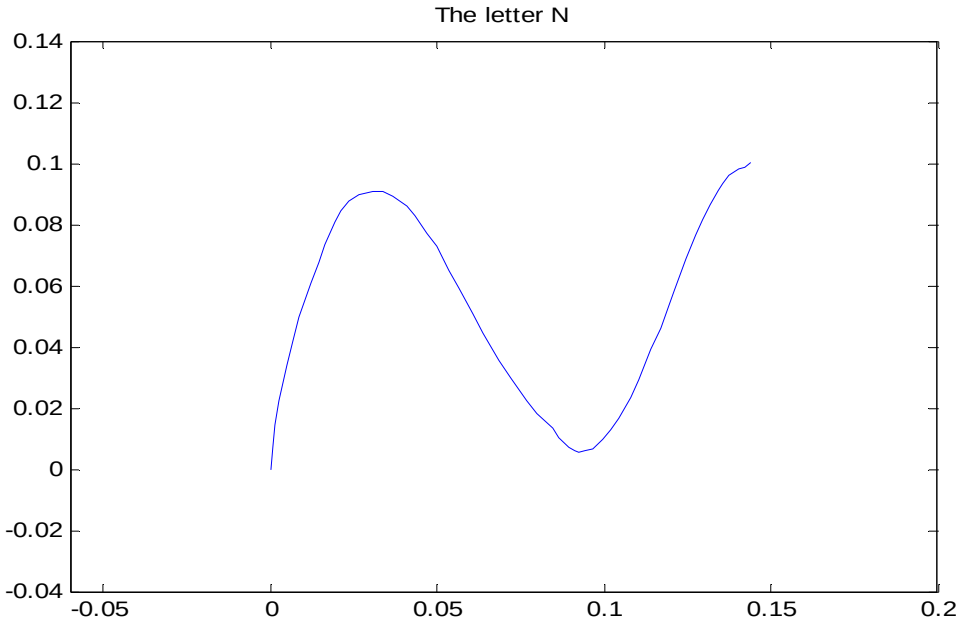

Figure 37. The Handwriting Trajectory of the Letter N, with the horizontal and vertical axis units in meters.

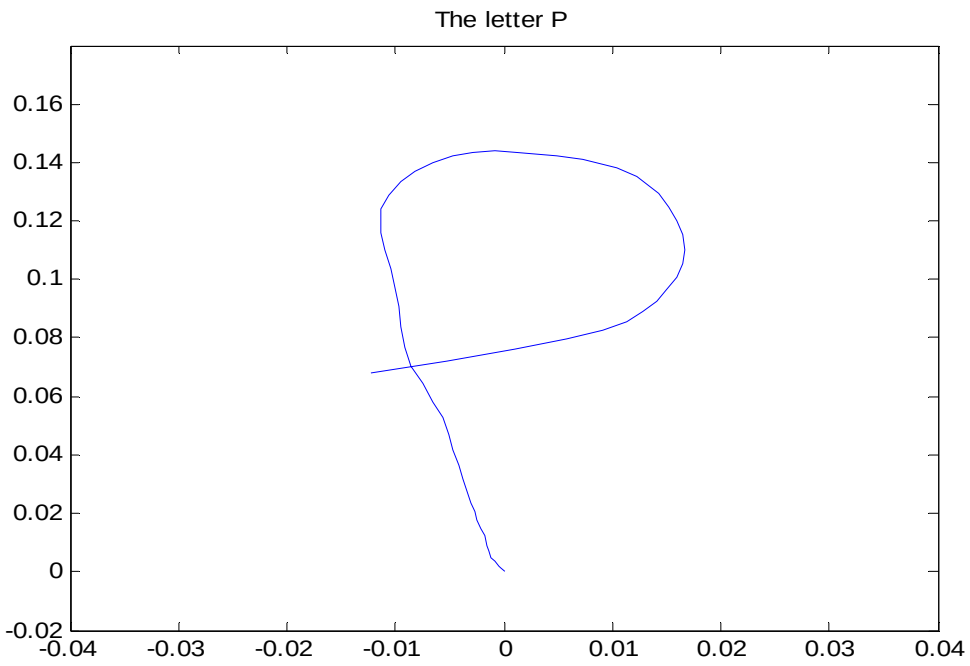

Figure 38. The Handwriting Trajectory of the Letter P, with the horizontal and vertical axis units in meters.

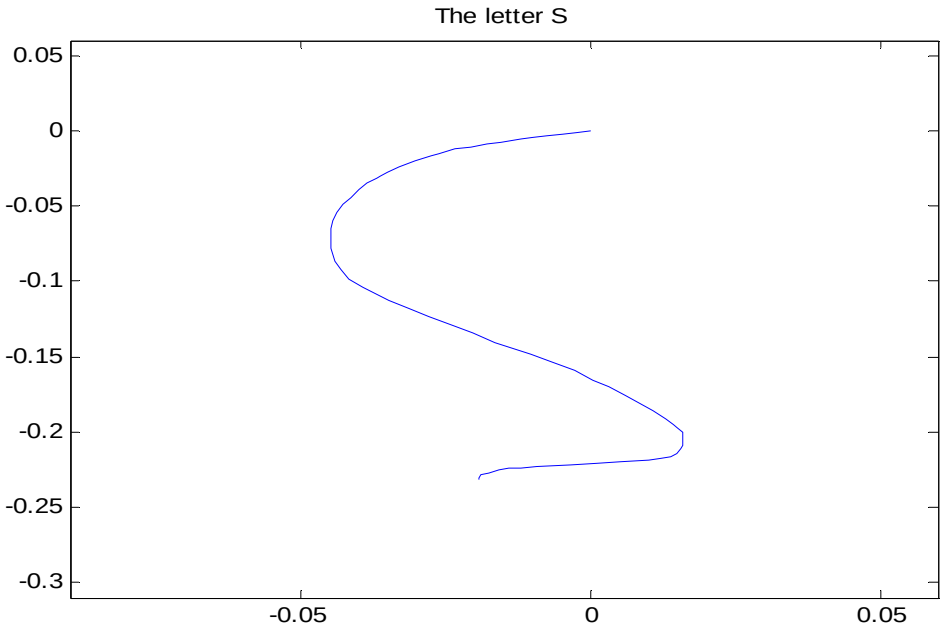

Figure 39. The Handwriting Trajectory of the Letter S, with the horizontal and vertical axis units in meters.

Figures 40, 41, 42, 43, 44, 45, 46, 47, 48, and 49 are the reproduced handwriting trajectories of the numbers 1 to 10.

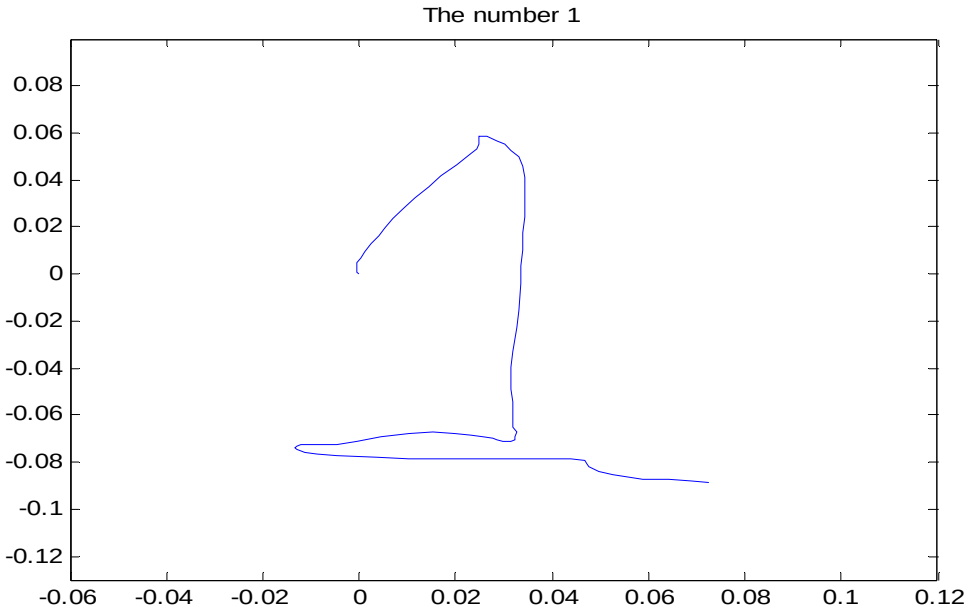

Figure 40. The Handwriting Trajectory of the Number 1, with the horizontal and vertical axis units in meters.

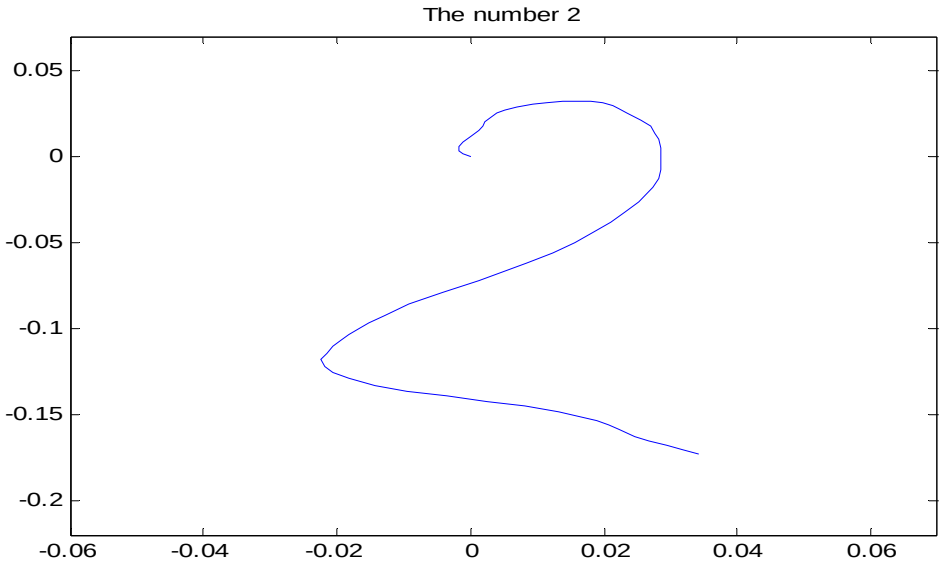

Figure 41. The Handwriting Trajectory of the Number 2, with the horizontal and vertical axis units in meters.

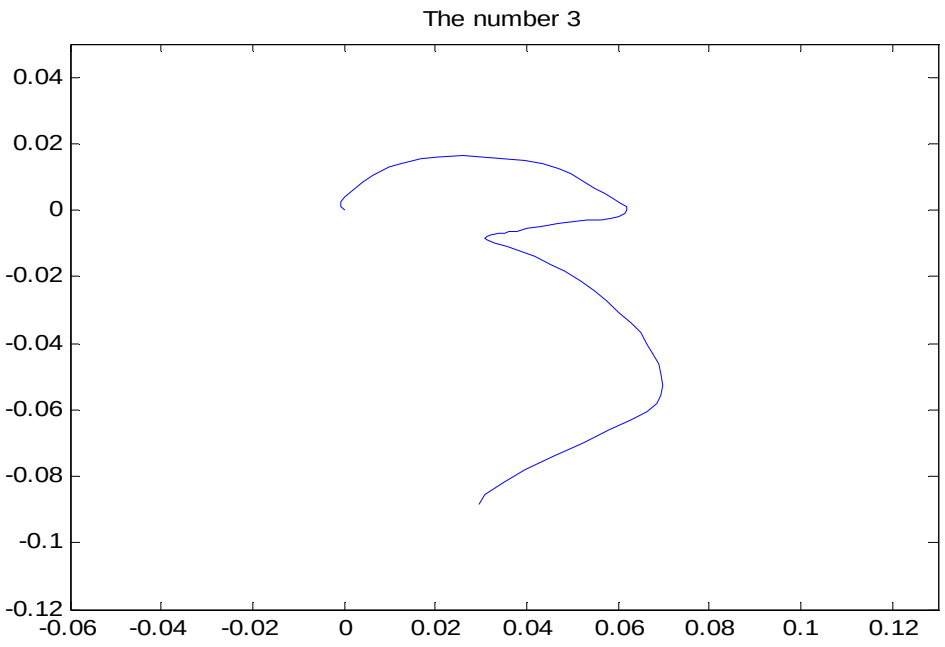

Figure 42. The Handwriting Trajectory of the Number 3, with the horizontal and vertical axis units in meters.

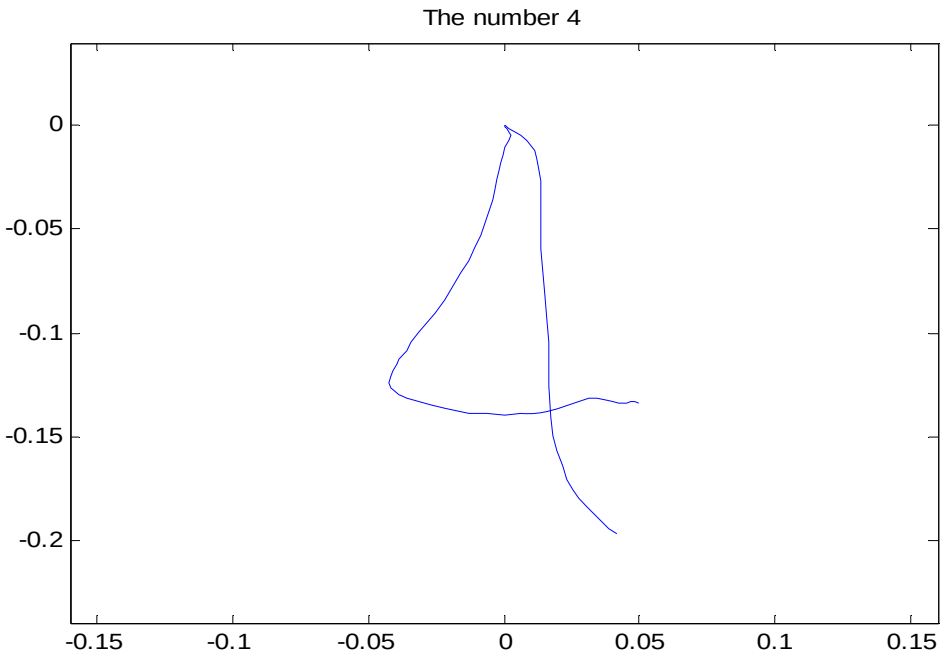

Figure 43. The Handwriting Trajectory of the Number 4, with the horizontal and vertical axis units in meters.

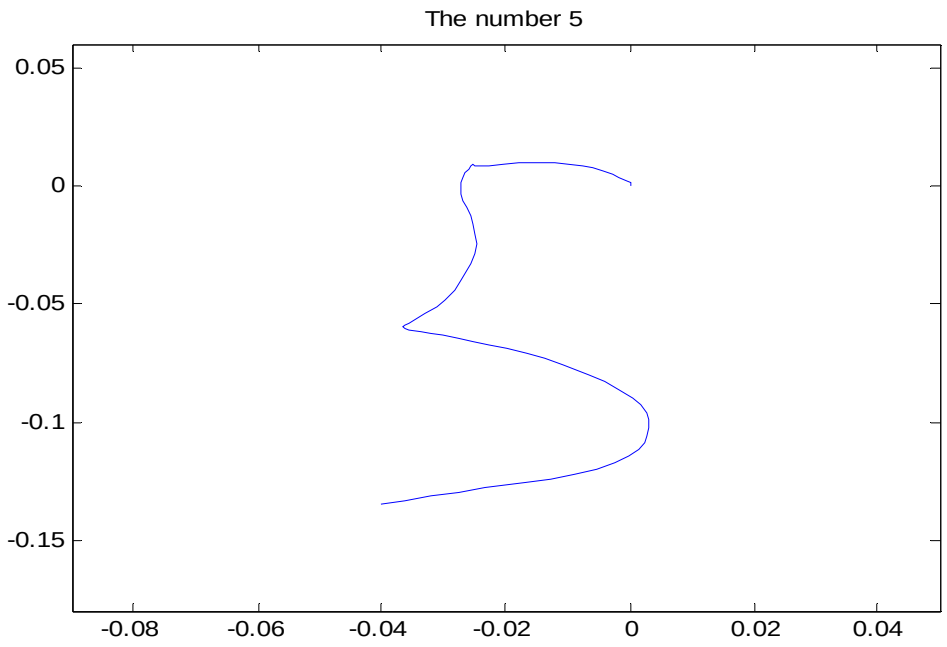

Figure 44. The Handwriting Trajectory of the Number 5, with the horizontal and vertical axis units in meters.

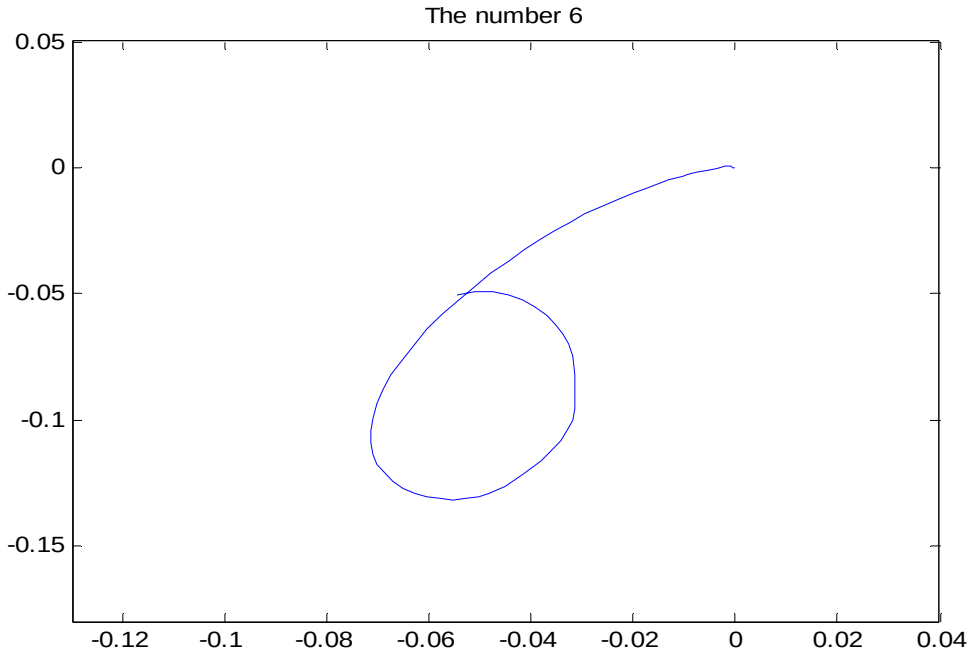

Figure 45. The Handwriting Trajectory of the Number 6, with the horizontal and vertical axis units in meters.

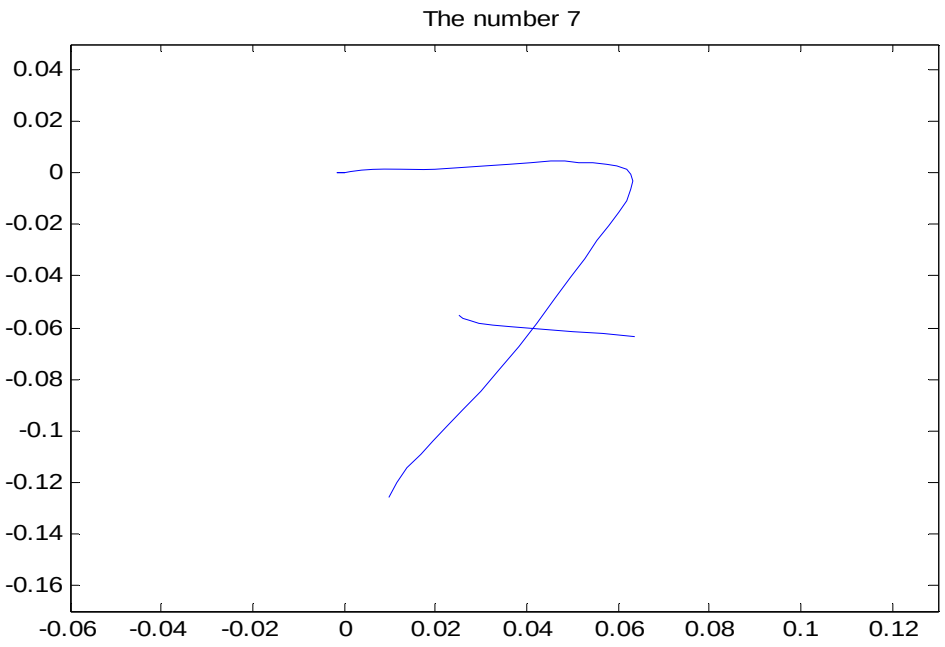

Figure 46. The Handwriting Trajectory of the Number 7, with the horizontal and vertical axis units in meters.

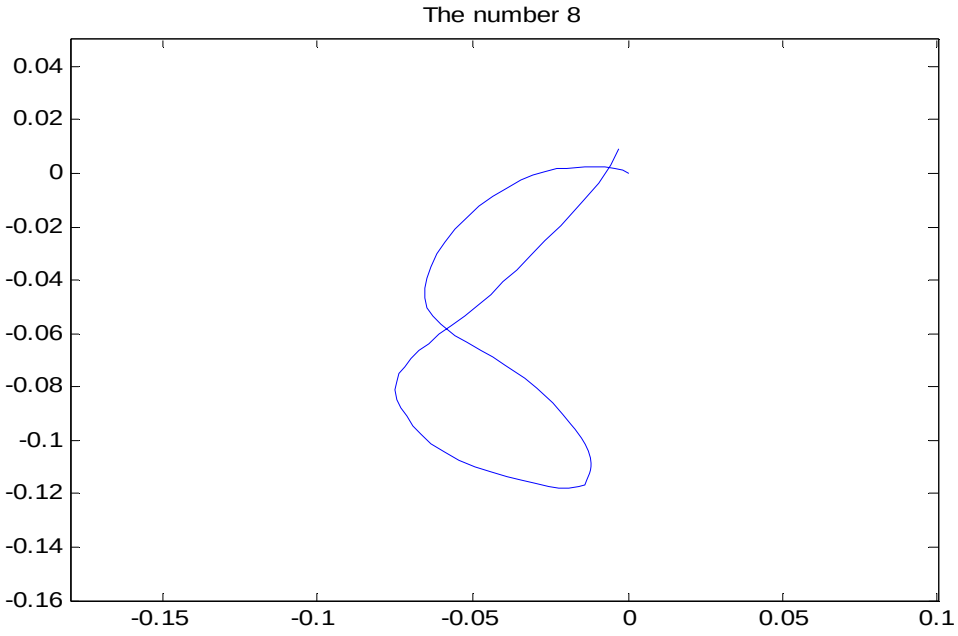

Figure 47. The Handwriting Trajectory of the Number 8, with the horizontal and vertical axis units in meters.

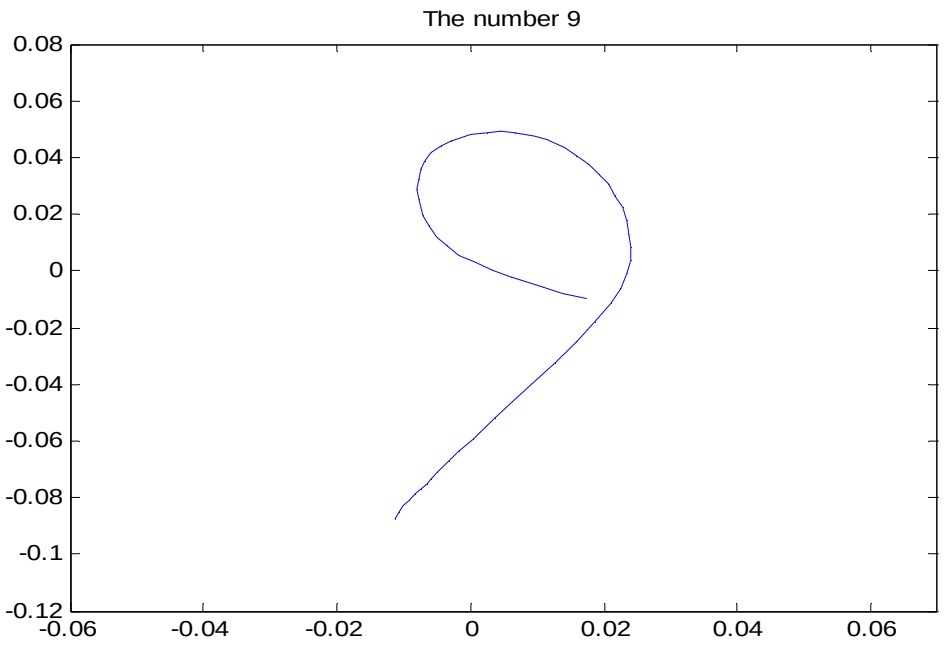

Figure 48. The Handwriting Trajectory of the Number 9, with the horizontal and vertical axis units in meters.

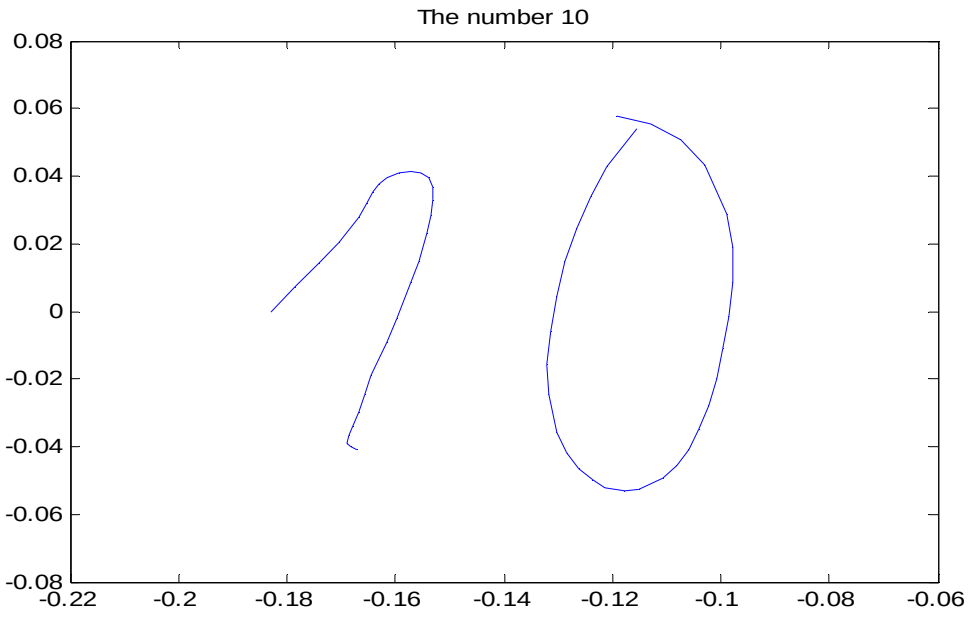

Figure 49. The Handwriting Trajectory of the Number 10, with the horizontal and vertical axis units in meters.

For the reasons explained in Chapter V, in this main algorithm the beginning and the end points of each stroke, are also found and the velocity correction algorithm and then the integration of the corrected velocity are implemented separately for each stroke.

Figure 50 presents the handwriting trajectory of the acronym NPS by tracking this word with the pen input device.

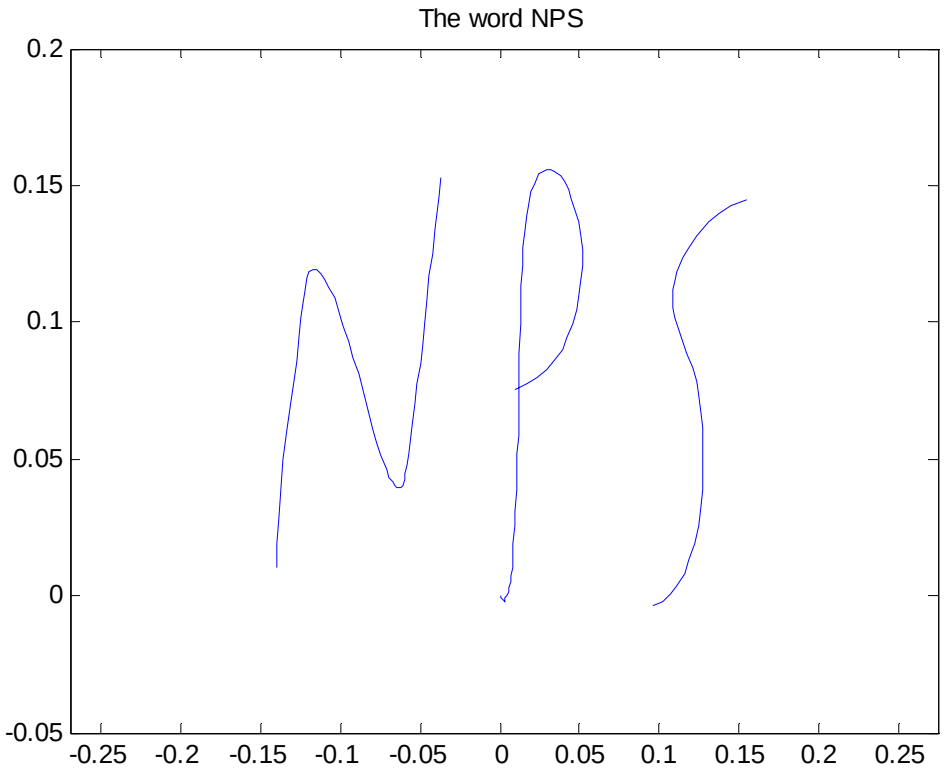

Figure 50. The Handwriting Trajectory of the Acronym NPS, with the horizontal and vertical axis units in meters.

Figure 50 indicates that the pen input device can be used for the reproduction of handwriting trajectories not only for letters but also for words as well as sentences.

Chapters V and VI presented experimental handwriting results of alphanumeric characters in 2-D space and 3-D plane. All the matlab code that was used in this thesis research is available to Professor Yun Xiaoping. The next chapter summarizes the research conducted in this thesis, and provides recommendations for future work.

VII. CONCLUSION AND RECOMMENDATIONS

A. CONCLUSION

In this thesis research, the feasibility of a pen input device that can reproduce the handwriting trajectory of alphanumeric characters using an inertial/magnetic sensor module was investigated.

This research was started with an experiment demonstrating the importance of the sensor velocity for the reproduction of an accurate handwriting trajectory. The sensor was placed in a 2-D plane and moved to track a straight line with three different velocities. The numerical and graphical results indicated that the high sensor velocity is crucial for reproducing handwriting trajectory.

In this thesis, a calibration algorithm was also studied. The calibration algorithm was computed the constant length vector between the nose of the pen input device and the point where the inertial/magnetic sensor was attached to the pen. In this research, the sensor was attached at a pen in a distance of 14 cm from the nose of the pen. After the implementation of the equations that described in Matlab, the constant length was computed to be 14.1 cm.

A velocity correction algorithm was also described in this thesis. An experiment with the sensor indicated that prior to the sensor motion and after the sensor motion, the sensor velocity was nonzero. The nonzero data in the velocity result in an error or drift and grows along with the time. Mathematical equations were applied for eliminating that error and after the implementation of them in Matlab, an accurate handwriting trajectory was accomplished.

Experimental handwriting results of alphanumeric characters for handwriting tracking in 2-D plane and 3-D space were presented in this thesis research. It is observed from all the handwriting results that the reproduced handwriting trajectories are qualitatively correct and recognizable by humans. This indicates that the construction of this pen input device using an inertial/magnetic sensor for the reproduction of the

handwriting trajectory of alphanumeric characters to a 2-D plane can be feasible. However, the inaccurate handwriting trajectories result from the inaccurate quaternion provided from the sensor and the speed of the writing motion.

As explained in Chapter II, the sensor provides accurate acceleration data and consequently an accurate handwriting trajectory only by using the sensor with high motion velocity. As mentioned in Table 1 of Chapter II, the handwriting trajectory of a straight line has the smaller distance error for the sensor motion velocity around 42.4 cm/sec. However, the performance of tracking alphanumeric characters in a 2-D plane and 3-D space with a sensor motion velocity around 40cm/sec to 50cm/sec is really difficult and sometimes infeasible, especially for complicated alphanumeric characters. Apart from that, the handwriting tracking is not accurate with such a writing speed, and consequently the sensor does not collect accurate data for the alphanumeric characters. Hence, the sensor does not provide the accurate acceleration data which leads to errors in the double integration and consequently an inaccurate handwriting trajectory is reproduced.

Many times it was explained and implemented in this thesis research that the quaternion is necessary for the conversion of the acceleration measurements from the sensor coordinate system into the earth coordinate system by using Equation (9) from chapter III. This conversion is necessary because the position of the nose of the pen must be calculated in the earth coordinate system as explained in Chapter I. It is obvious that errors in the quaternion will affect the accuracy of the acceleration data in the earth coordinate system.

The sensor specifications as described in [3], state that the dynamic accuracy of the sensor is +/- 2 degrees for arbitrary orientation angles. That indicates that the sensor does not provide the accurate orientation quaternion and thus of the pen while the handwriting tracking is taking place. Therefore, the inaccurate quaternion creates errors in the acceleration data and accordingly after the double integration to the handwriting trajectory.

Apart from that, the performance of handwriting tracking of alphanumeric characters using the factored quaternion algorithm (FQA) was also tested instead of the quaternion provided from the sensor. However, the handwriting results were unacceptable and unrecognizable.

This was expected because the computation of the quaternion from the factored quaternion algorithm as described in [4] is based only on the measured acceleration and magnetometer data as. The FQA [4] implements equations for the computation of the quaternion using the measured acceleration and magnetometer data. However, it is known from Chapter II that the sensor did not provide accurate acceleration data for a normal hand's motion velocities.

Hence, it is obvious that the FQA [4] provided the quaternion with a bigger error than the sensor quaternion for its motion because it depends only on the inaccurate acceleration measurements. For that reason, the FQA was used only in the calibration algorithm as stated in Chapter III because handwriting tracking and consequently the sensor motion was not taking place.

B. RECOMMENDATIONS

For the conclusions explained above, it is recommended that the accuracy of the handwriting trajectory can be improved by using a different kind of inertia/magnetic sensor. It is suggested to use an inertia/magnetic sensor that can provide accurate acceleration data to slower and normal hand motion velocities.

It is also recommended for the improvement of the accuracy of the quaternion an algorithm that can be more effective than the factored quaternion algorithm (FQA) be developed.

Finally, it is recommended the use and test of the pen input device be conducted by multiple users.

THIS PAGE INTENTIONALLY LEFT BLANK

APPENDIX

The following specifications for the inertial/magnetic sensor module MicroStrain 3DM-GX1 that was used in this thesis research are from reference [3].

Orientation Range	360˚ full scale (FS), all axes (Matrix, Quaternion modes)
Sensor Range	Gyros: 300˚/sec FS; accelerometers: 5 G's FS; magnetometers: 1.2 Gauss FS
A/D Resolution	16 bits
Accelerometer Nonlinearity	0.2%
Accelerometer Bias Stability*	0.010 G's
Gyro Nonlinearity	0.2%
Gyro Bias Stability*	0.7˚/sec
Magnetometer Nonlinearity	0.4%
Magnetometer Bias Stability*	.010 Gauss
Orientation Resolution	< 0.1˚ minimum
Repeatability	0.20˚
Accuracy	0.5˚ typical for static test conditions, 2˚ typical for dynamic (cyclic) test conditions and for arbitrary orientation angles
Output Modes	Matrix, Quaternion, Euler angles and 9 scaled sensors with temperature
Digital Outputs	Serial RS-232 and RS-485 optional with software programming
Analog Output Option	0-5 volts FS for Euler angles (pitch 90, roll 180, yaw 360˚)
Digital Output Rates	100 Hz for Euler, Matrix, Quaternion; 350 Hz for nine orthogonal sensors only
Serial Data Rate	19.2/38.4/115.2 Kbaud, software programmable
Supply Voltage	5.2 VDC min., 12 VDC max.
Supply Current	65 milliamps
Connectors	One keyed LEMO, two for RS-485 option
Operating Temperature	-40˚ to +70˚ C with enclosure; -40˚ to +85˚ C without enclosure
Size with Enclosure Size without Encl.	65 x 90 x 25 mm 2.5 x 3.5 x 1.0" 42 x 40 x 15 mm; 1.65 x 1.6 x 0.6"
Weight	74.6 gr. with enclosure, 25.8 gr. without enclosure
Shock Limit	1000 G's (unpowered); 500 G's (powered)

**Accuracy and stability specifications obtained over operating temperatures of -40˚ to +70˚ C with known sine and step inputs, including angular rates of 300 degrees per second.*

THIS PAGE INTENTIONALLY LEFT BLANK

LIST OF REFERENCES

[1] "Ultrasound position input device," last accessed November 2008, http://www.freepatentsonline.com/4814552.html.

[2] "Electronic pen device," last accessed November 2008, http://www.freshpatents.com/Electronic-pen-device-dt20080710ptan20080165162.php.

[3] "3DM-GX1 MicroStrain AHRS Orientation Sensor," last accessed March 2008, http://www.microstrain.com/3dm-gx1.aspx.

[4] Xiaoping Yun, Eric R.Bachmann, and Robert B.McGhee, "A simplified Quaternion-based algorithm for orientation estimation from Earth gravity and magnetic field measurements," IEEE Transactions on Instrumentation and Measurement on Volume 57, Issue 3, March 2008: pp. 638-650.

[5] H.Moore, "Networked humanoid avatar driven by marg sensors," Master's thesis, Naval Postgraduate School, Monterey, California, September 2006.

[6] Won-Chul Bang, Wook Chang, Kyeong-Ho Kang, Eun-Seok Choi, Alexey Potamin, and Dong-Yoon Kim, "Self – contained Spatial Input Device for wearable computers," Proceedings of Seventh IEEE International Symposium on Wearable Computers, 21-23 October 2003: pp. 26-34.

[7] X.Yun, "Kinematic equations of a 3-D input device using IMUs," Research Notes, Naval Postgraduate School, July 2008.

THIS PAGE INTENTIONALLY LEFT BLANK

INITIAL DISTRIBUTION LIST

1. Defense Technical Information Center
   Ft. Belvoir, VA

2. Dudley Knox Library
   Naval Postgraduate School
   Monterey, CA

3. Chairman, Code EC
   Department of Electrical Engineering
   Naval Postgraduate School
   Monterey, CA

4. Xiaoping Yun
   Department of Electrical Engineering
   Naval Postgraduate School
   Monterey, CA

5. Roberto Cristi
   Department of Electrical Engineering
   Naval Postgraduate School
   Monterey, CA

6. Marcello Romano
   Department of Mechanical Engineering
   Naval Postgraduate School
   Monterey, CA

7. James Calusdian
   Department of Electrical Engineering
   Naval Postgraduate School
   Monterey, CA

8. Leonidas Drakopoulos
   Department of Electrical Engineering
   Naval Postgraduate School
   Monterey, CA